Quantum Chemical Investigations on Acetylenic Carbon Rich Compounds as Molecular Construction Kit

By

Mustafa AYDIN

A Dissertation Submitted to the Graduate School in Partial Fulfillment of the Requirements for the Degree of

MASTER OF SCIENCE

Department: Chemistry

Major: Chemistry

İzmir Institute of Technology

İzmir, Turkey

September, 2004

We approve the thesis of **Mustafa AYDIN**

Date of Signature

…….. **10.09.2004**

Assoc. Prof. Dr. Nuran ELMACI

Supervisor

Department of Chemistry

……..... **10.09.2004**

Prof. Dr. Levent ARTOK

Department of Chemistry

…….. **10.09.2004**

Prof. Dr. Recai ERDEM

Department of Physics

…….. **10.09.2004**

Assoc. Prof. Dr. Ahmet E. EROĞLU

Head of Department

ACKNOWLEDGEMENTS

I would like to express my sincere gratitude to my advisor, Assoc. Prof. Nuran ELMACI, for her supervision, guidance, support, and encouragement.

I would like to appreciate deeply to my roommates, research assistants: Türker PASİNLİ, Öznur KAFTAN, Bahar ÖZMEN, Aytaç ŞAHİN, and Betül ÖZTÜRK.

Finally, I would like to thank my family for their support, encouragement, and understanding.

ABSTRACT

Ground and excited state behaviors of Radialenes, Expanded Radialenes and TEE monomer and dimer derivatives, which are carbon rich compounds were investigated by using quantum chemical calculations. Most of these advanced materials have non-linear optical properties and they can be used as molecular electronics.

AM1 and DFT/B3LYP with 3-21G and 6-31G* basis sets methods were used for the ground state calculations of radialenes, expanded radialenes and TEE monomers and dimers. TDDFT/3-21G, TDDFT/6-31G* level of calculations were carried out for the excited state behaviors on AM1, DFT/3-21G* and DFT/6-31G* ground state structures. All the methods that we have used gave similar results with a very small discrepansies.

Radialenes and expanded radialenes have planar ground state structures except the one with size 6; the three dimensional chair like geometry is slightly stable than the planar one. There is no effect of the size of radialenes on the the geometrical parameters. The introduction of ethynyls instead of hydrogens causes a red-shift about 100-150 nm. The maximum absorption wavelength usually increases with the size of radialenes with some exceptions for the planar structures.

The effect of various acceptors such that p-NO_2-benzene- , p-CH_3-benzene-, p-CHO-benzene- and their locations which are mainly CIS, TRANS and GEMINAL with respect to donor positions to the TICT state on push-pull TEE derivatives were investigated by using excited state calculations. The probable donor units on the TEE derivates were considered as dimethyl amine and dimethyl aniline units. TICT property for the rotation of dimethylaniline group is observed for many of isomers. TICT state appeared both for cis and trans conformer of the donor substituted TEE dimer.

ÖZ

Karbonca zengin asetilenik bileşikler olan TEE monomeri ve dimerinin türevleri, radyalinler ve genişletilmiş radyalinlerin temel hal ve uyarılmış hal davranışları kuvantum kimyasal yöntemlerle incelendi. Adı geçen bu ileri malzemelerin lineer olmayan optik özellikleri yüksek olup moleküler elektronik olma potansiyeline sahip olduğu bilinmektedir.

Hesaplarımızda Gaussian-98 programının kapsamında olan AM1 ve DFT, TDDFT yöntemleri kullanıldı. DFT'de 3-21G* ve 6-31 G* bazları temel halde, uyarılmış halde ise TDDFT yöntemi 3-21G ve 6-31 G* bazlarıyla uygulandı. Kullandığımız hesaplama seviyeleri arasında çok büyük sonuç farkı gözlenmedi.

Halkalı bileşikler olan radyalinler ve genişletilmiş radyalinlerin temel hal yapılarının halka genişliği 6 olanları dışında düzlemsel olduğu altılılarda ise çok az enerji farkıyla 3 boyutlu sandalye konformasyonunun daha kararlı yapıda bulunduğu gözlemlendi. Halka genişliğinin yapısal parametrelere etkisi olmadığı belirlendi. Halka dışındaki uç hidrojenler yerine etinil takıldığında 100-150 nm kırmızı kayması görüldü. Düzlemsel yapılar düşüldüğünde halka genişliği arttıkça maksimum dalga boyunun da genel olarak arttığı saptandı.

Alıcı grubunun dimetilanilin(DMA) takıntılı TEE monomerinin temel hal ve uyarılmış hallerine ve burkulmuş molekül içi yük transferi haline (TICT) etkisi çeşitli alıcı gruplar kullanılarak incelendi, kullanılan gruplar p-NO_2-benzen- , p-CH_3-benzen- ve p- CHO-benzen-dir. Ayrıca bu grupların yer etkisi de vericiye göre CIS, TRANS ve GEM pozisyonları kullanılarak incelendi. TEE üzerindeki olası verici gruplar DMA ve Dimetilamin olarak ele alındı. Alıcı grubun kuvveti arttıkça maksimum dalga boyunun arttığı gözlendi. TICT hali cis ve trans izomerlerinde DMA grubunun burkulmasında açıkça görülmektedir. TEE dimerinde ise her iki izomer için de, sonuçlarımız TICT halinin varlığını göstermektedir.

TABLE OF CONTENTS

LIST OF TABLES

LIST OF FIGURES

CHAPTER I

INTRODUCTION

1.1. Introduction

During the past decade, scientists have become increasingly interested in the preparation of polymeric carbon allotropes and carbon-rich nanometer-sized compounds that have been proposed based on theoretical calculations and synthesis. These compounds display desirable characteristic, such as unusual structures, high stability, and superior electronic and nonlinear optical properties [1]. These properties can be tunable by synthesis.

For the construction of these materials of fundamental and technological interest at the interface between chemistry and materials science, scientists developed a large molecular construction kit of building blocks, which are one, two, and three dimensional networks. Many of these carbon rich designer materials are constructed from acetylenic building blocks, and several of them will be the subjects of this study.

Acetylenic scaffolding with derivatives of tetraethynylethene (TEE, 3,4-diethynylhex- 3-ene-1,5-diyne) and radialenes provides carbon-rich compounds with interesting physicochemical properties. Thus, these modules are building blocks for monodisperse, linearly π-conjugated oligomers [polytri(acetylene)s, PTAs] extending in length beyond 10 nm, and for large, macrocyclic, all-carbon cores (expanded radialenes) exhibiting strong chromophoric properties [2,3].

In following sections, we will mention briefly carbon-rich compounds, its applications and studies.

1.2. Acetylenic Carbon-Rich Compounds

We can classify Carbon-Rich Acetylenic Compounds (CRAC) into two parts; Acyclic and cyclic Carbon-Rich Compounds

1.2.1 Acyclic Acetylenic Carbon-Rich Compounds

Tetraethynylethene (**1**) and its derivatives represent a class of two-dimensionally conjugated building blocks with reported potential as precursors to carbon-rich nanometer-sized compounds with unusual structures, high stability, and useful electronic and nonlinear optical properties [1,4]. The first member of this class is tetrakis(phenylethynyl)ethene (**2**). It was discovered by *Hori* et al in 1969 [5]. Several years later persilylated derivative was synthesized by *Hauptmann* [6-8]. A synthesis of the parent unprotected molecule **1** was first reported by *Diederich* and coworkers in 1991 [9].

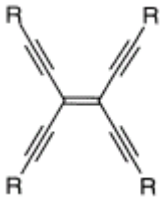

1 R=H

2 R=Ph

Figure 1.1. TEE and The first derivatives of TEE

Since then, the chemistry of TEEs has improved considerably, so that now synthetic routes to virtually any desired protection and substitution pattern about the central ten carbon core have been achieved [10-12]. The synthetic flexibility inherent to these systems has allowed them to function as a "molecular construction kit" for the preparation of acyclic [13] and macrocyclic acetylenic compounds [14-17] as well as for polymerization into rod-like linear oligomers and polymers with the conjugated polytriacetylene (PTA) backbone like **3** [18-22]. PTA oligomers and polymers **(4)** have

also been constructed starting from 1,2-diethynylethenes (DEEs, hex-3-ene-1,5-diynes).[3,23]

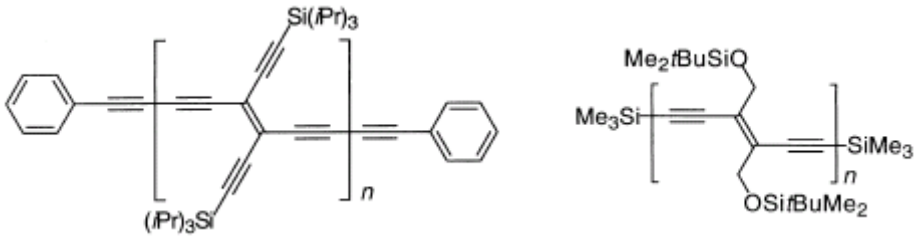

3 **4**

Figure1.2. The examples for PTA oligomers.

Electron donating and electron accepting functionality have been attached to the planar TEE chromophore to increase the appeal of TEEs as potential materials for electronics and photonics. The expanded, conjugated eneyne carbon cores of functionalized TEEs are ideal for studying conjugation effects because, in contrast to similar structures such as cis-stilbenes [24] and tetraphenylethenes [25], TEEs have a fully planar, simple framework. The aryl rings with donor or acceptor (D/A) functionalities are sufficiently remote from each other as to prevent unfavorable steric interactions, and thus electronic effects can be isolated from steric influences. X-ray structural analyses of several silyl- and D/A-substituted arylated TEEs have shown that nearly perfect planarity is maintained across the entire conjugated π skeleton including the aryl rings. [9,10], [26-28]

The attachment of the various substituents to the planar TEE backbone, different conjugation pathways appear. One-dimensional linear *trans*- or *cis*-donor-acceptor conjugation (pathways (a) and (b)) as shown in Figure1.3 is much more effective than geminal substitution cross conjugation (pathway (c)). With functional groups attached at all four ends, a total of six conjugation pathways provide a complete, two-dimensional conjugation combining two linear *trans*-conjugation (a), two linear *cis*-conjugation (b), and two geminal cross conjugation (c) paths.

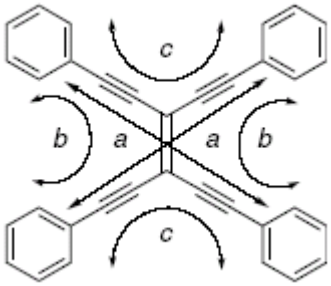

Figure1.3. The phenyl-substituted TEE is planar, [28] thereby allowing for full two-dimensional conjugation. Paths *a* and *b* depict *trans*- and *cis*-linear conjugation, whereas path *c* depicts geminal crossconjugation.

The extent of π-conjugation (linear, cross, or two dimensional conjugation), the degree of functionalization (mono-, di-, tri-, or tetra-substitution), and the donor-acceptor strength manage molecular properties such as electronic absorption, [26,27] luminescence, [26,27] redox behaviour, [29,30] and nonlinear optical responses [31,32] in these highly conjugated TEE chromophores. The UV/V spectra of donor-acceptor substituted TEEs reveal a bathochromic shift of the longest wavelength band (λ_{max}) with (i) changing from geminal orientation of the substituents to cis and trans linear conjugation pathways, (ii) increasing conjugation length, and (iii) increasing the number of trans-donor-acceptor pathways upon tetrakisfunctionalization, in other words generation of two-dimensional conjugation [26,27]. Furthermore, TEE derivatives are attractive compounds for nonlinear optical (NLO) materials on account of their intrinsic two-dimensional π-electron conjugation pathways. Indeed, donor-acceptor-substituted TEEs display some of the highest known third-order nonlinearities. The third-order nonlinear optical coefficients γ are raised by increasing (i) the degree of donor substitution, (ii) the donor strength, (iii) the length of the conjugation path, and (iv) the number of linear donor-acceptor conjugation pathways in the molecules, i.e. full two dimensional conjugations strongly enhances γ. They also show very large second-order NLO effects.

The optical spectra of donor-acceptor substituted derivatives displayed characteristic long-wavelength bands resulting from intramolecular charge transfer.The absorption spectra of the anilino-substituted compounds display broad absorption

shoulders at low energy (λ_{max} in the range 550–580 nm) and with end absorptions extending to 600 nm and beyond. These bands were assigned to charge-transfer (CT) transitions from the electron-donating anilino groups to the central carbon core. Indeed, this CT transition was lost for each dimer when the anilino groups were protonated with concentrated aqueous HCl [35]. These results imply that the central conjugated C_{20} core in the TEE dimers, with its 16 C(sp) atoms, is a strong electron acceptor. It concludes that the chromophoric properties of TEE dimers are readily tunable: upon suitable functionalization, their absorption region can be expanded close to the near IR absorption range [36].

1.2.2 Cyclic Acetylenic Carbon-Rich Compounds

1.2.2.1. Radialenes

The all-exo-methylenecycloalkanes represent the first members of a homologous series of compounds with the general formula C_nH_n. In contrast to their constitutional isomers with endocyclic, linearly conjugated double bonds such as benzene and cyclooctatetraene, the radialenes possess an uninterrupted cyclic arrangement of cross-conjugated π systems. They are alicyclic hydrocarbons in which all ring carbon atoms are sp^2-hybridized and which carry as many semicyclic double bonds as possible.

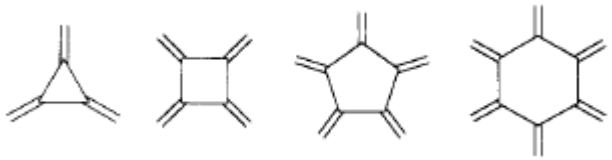

Figure 1.4. The series of Radialenes **(**exo-methylenecycloalkanes)

Radialenes are a recent class of compounds. Hexaethylidenecyclohexane was the first reported and H. Hopff published its synthesis in 1961. The derivative of [3]radialene, Triisopropylidenecyclopropane was first described in 1965 [37]. [3]radialene [38] and [4]radialene [39] were prepared in 1965, and for [6]radialene

three independent syntheses were reported in 1977/78 [40,41] . [5]radialene is of much interest especially after the discovery of fullerene (C60) in 1985 because it is the formal "monomer" of fullerene. A derivative of [5]radialene was obtained in 1986. The radialenes, which are cross-conjugated systems, have always been overshadowed by the linearly conjugated polyenes and the arenes in preparative and industrial organic chemistry. However, in recent years interest in this class of compounds has increased significantly because new methods of synthesis make radialenes more accessible, and they are potential candidates for the construction of organic conductors and ferromagnets.

The highly symmetrical structure of these compounds suggested by their constitutional formulas is so attractive. So these regular structures with the double bonds "radiating" from the central ring led to the name "radialene(s)". Thus general term for the parent molecules is [n]radialenes (n = 3, 4, 5, 6) where n stands for the ring size and , the number of the exocyclic double bonds.

According to electron diffraction measurement as well as IR and Raman spectra, [3]radialene is planar molecule with D_{3h} symmetry. [4]Radialene posses a planar cyclobutane ring as long as there is no steric strain between substituents. The chair-type conformation of the sterically hindered hexakis(ethylidene)cyclohexane seems to indicate that the parent molecule [6]radialenes prefers this conformation as well. For [5]radialenes, steric hindrance between the substituents does not allow a planar radialene skeleton [42].

The simple radialenes [3]-, [4]-, [5]-, and [6]-radialene are very unstable in air. They polymerize at room temperature [45]**.** The [3]-, [4]-, and [6]-radialenes have been produced at low temperatures, but [5]-radialene has not been synthesized in our knowledge. Despite the instability of the parent compounds, many stable derivatives exist [8].

The cyclic arrangement of the π systems of the radialenes led to early speculations on whether in these molecules a stabilizing or destabilizing cyclic electron delocalization was present. Numerous theoretical investigations involving especially π resonance energies, total π electron density indexes, and the absolute and relative hardness as criteria have been concerned with this problem. One result from these studies is that all radialenes are nonaromatic. The occurrence of localized endocyclic single bonds and exocyclic double bonds, as indicated by many calculations as well as

structral studies, in addition to the nonplanarity of the substituted higher radialenes clearly speak against the delocalization of the π-electron density [44].

Radialenes and their derivatives have recently been receiving growing attention from preparative chemists, spectroscopists, and materials scientists [42,43].The introduction of polarizing substituents can converts radialenes into novel π-donors and π-acceptors, of interest, for the preparation of novel charge transfer complexes [45]. Recently, radialenes have been employed in molecular scaffolding [15].

1.2.2.2. Expanded Radialenes

The carbon-rich homologous series of expanded radialenes with the molecular formulate $C_{2n}H_n$ and $C_{3n}H_n$, respectively, are obtained [16]. They are a family of macrocycles derived from radialenes [42] upon formal insertion of ethynediyl or buta-1,3-diynediyl moieties into the cyclic framework between each pair of vicinal exo-methylene units.

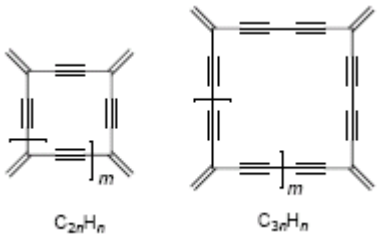

Figure 1.5. The series of Expanded Radialenes

The development of a number of synthetic strategies for preparing differentially silyl-protected TEEs [15,16] provided suitable modules for the construction of the first series of perethynylated-expanded radialenes. As precursors for expanded radialenes, it is employed geminally substituted TEEs as well as TEE-dimers, affording the perethynylated derivatives.

Among the macrocyclic scaffolds are perethynylated-expanded radialenes with large all-carbon cores extending up to C_{120}, which are potential precursors to fascinating 2D and 3D all-carbon networks. The first X-ray structural characterization of an expanded radialene as well as the redox properties and third-order nonlinear optical

properties of these unusual macrocycles were reported. For the all-carbon core with 60 C-atoms, an isomer of Buckminsterfullerene C_{60}, X-ray crystal structure analysis of this compound revealed that the cyclic core adopts a nonplanar, "chair-like" conformation [35].

The all-carbon cores of these novel macrocycles shown in figure1.6 can be viewed as isomers of C_{40} (expanded [4]-radialene 1), C_{50} (expanded [5]-radialene 2), and C_{60} (expanded [6]-radialene 3).

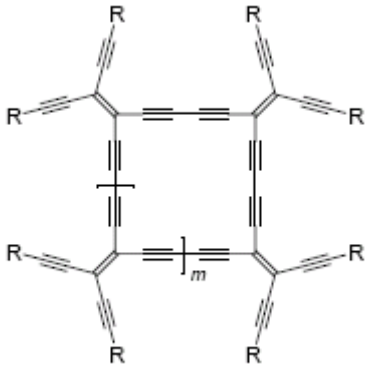

m = 1:

$C_{40}R_8$

m = 2:

Figure 1.6. As building blocks for the construction of expanded radialenes with peripheral functional groups (Perethynylated expanded radialenes)

The expanded [8]-radialene, with a C80 core, is the largest member of this new class of macrocyclic chromophores prepared so far. The materials properties of the expanded radialenes could be greatly enhanced upon donor functionalization with fully planar, conjugated π-chromophores. These compounds exhibit large third-order nonlinear optical coefficients can be reversibly reduced or oxidized and form monolayers at the air/water interface [22]. The electronic absorption spectrum of the trimeric of them displays a strong low-energy absorption band in the visible region with an exceptionally large molar extinction coefficient (ε = 171 000 dm^3/cm/mol at λ_{max} = 646 nm). The origin of this remarkable absorption is not yet well understood. [46]

Macrocyclic cross-conjugation is very efficient in expanded radialenes featuring peripheral aryl donor substituents. The measured bathochromic shifts of the absorption onset as a result of this conjugation are much larger than those observed in acyclic

cross-conjugated systems. This can be explained by the greater rigidity of the cyclic π perimeters, allowing better cross conjugative and homoconjugation-like orbital overlap.

Recent studies clearly demonstrate the importance of developing novel organic structures with extended π chromophores. Physical investigations of these compounds provide fundamental new insight into mechanisms of π -electron delocalization, as shown by the clear demonstration of donor-acceptor-enhanced macrocyclic cross-conjugation effects. In addition, promising advanced materials properties are created as demonstrated by the huge third order nonlinear optical coefficients of the donor-substituted perethynylated expanded radialenes. Efficient electron delocalization via cross-conjugation was instead accomplished in expanded radialenes containing electron donating substituents [47]. These macrocyclic chromophores exhibit strong and low-energy charge transfer transitions. And the cyclic cross-conjugated cores can better accommodate electrons than their linear counterparts.

1.3. In literature

The development of functional molecular architectures at the interfaces between chemistry and materials science as well as biology has now been successfully pursued by research groups especially Diederich group for more than 18 years. Molecules are designed and synthesized with the aim to express a desired function experimentally and theoretically. This function can be the specific optoelectronic property of an advanced material. Many of the target compounds feature dimensions on the multinanometer scale and could not have been prepared or characterized only 13 years ago. Rather, their successful development relies on recent advances in chemical synthesis, purification, and characterization. Moreover design strategies greatly benefit from enhanced computing power and the increasing availability of user-friendly computer modelling software. Thus, it becomes increasingly possible to correctly predict the 'active geometry', and the other properties for expression of function, of a target molecule.

In contrast, the synthesis of TEE ($C_{10}H_4$) was described in 1991 and, since then, a rich variety of cyclic and acyclic molecular architectures incorporating this carbon carbon-rich molecule as a construction module was prepared [12]. Diederich group revealed that the majority of these compounds, such as the expanded radialenes or the

oligomers and polymers of the poly (triacetylene) type, are highly stable and soluble and display a variety of interesting electronic and optical properties. In addition to the compounds that have been explicitly discussed many times [36,46,47], TEE molecular scaffolding has generated liquid crystalline PTA oligomers, solid state charge-transfer complexes with electrostatically controlled layered structures, and organometallic derivatives with TEE units as η^1-ligands coordinating to Pt centres.

Acyclic acetylenic scaffolding using both TEEs and DEEs afforded the first oligomers and polymers with the PTA backbone [20-23]. The effective conjugation length for this third class of linearly conjugated polymers with a nonaromatic all-carbon backbone was determined to be in the range of 7–10 monomeric units. One- and two-dimensional acetylenic scaffolding [49] with derivatized TEEs and DEEs provided access to advanced materials for electronic and photonic applications, such as chromophores with high second- and third-order optical nonlinearities; molecular photochemical switches; large, two-dimensional carbon cores and linearly p-conjugated molecular rods. Thus, the PTAs represent an important example of monodisperse molecular rods that was constructed by DEE or TEE monomer units [46, 47].

Donor-acceptor substituted arylated TEEs and DEEs were prepared, and their unusual electrochemical properties and tendency to undergo photochemical *trans*/*cis* isomerization were investigated as a function of structure, solvent, excitation wavelength, and temperature [26–28,50-52]. The *cis*-*trans* isomerism of arylated tetraethynylethenes has been exploited in the construction of sophisticated photochemically driven molecular switches. Measurements of third-order nonlinear optical effects by third harmonic generation revealed useful structure-function relationships. The highest second hyperpolarizabilities γ were obtained for two-dimensionally fully conjugated systems with reduced molecular symmetry [33,34].

Tetraethynylethene dimers and perethynylated-expanded radialenes were prepared in good yields by oxidative acetylenic coupling under Hay conditions by M. B. Nielsen et al. They employed two protocols for synthesizing the expanded radialenes: i) cyclization of TEE monomers, allowing isolation of [n]radialenes with n=3-5, or ii) cyclization of TEE dimers, allowing isolation of [n]radialenes with n=4, 6, or 8. It was included in this investigation the study of donor/acceptor-functionalized TEE dimers, which serve as model compounds to evaluate macrocyclic cross-conjugation effects in the expanded radialenes. And the physical properties of these two classes of compounds

were investigated by ^{1}H and ^{13}C NMR spectroscopy, electronic absorption, and emission spectroscopy, and electrochemistry. They also reported the first X-ray structural characterization of an expanded radialene as well as the redox properties and third-order properties of these unusual macrocycles [35].

These carbon- rich compounds also attracted the interest of theoreticians ab initio calculations have been carried out on the molecular and electronic structures of several acetylenic monomeric precursors. The equilibrium geometries of tetraethynylmethane (C_9H_4), tetraethynylethene ($C_{10}H_4$), tetraethynylallene ($C_{11}H_4$), tetraethynylbutatriene ($C_{12}H_4$), and hexaethynyl[3]radialene ($C_{18}H_6$), have been determined with the Hartree-Fock method using a double zeta plus polarization basis set. Good agreement between experiment and the calculated geometries have been achieved for the known $C_{10}H_4$, $C_{12}H_4$ and $C_{18}H_6$. For C_9H_4, however, the experimental triple bonds are considerably shorter (by 0.05 Å) and the $C(sp^3)$-C(sp) single bonds are slightly longer [53,54].

W. Rogers and J. McLafferty performed calculations at the G3(MP2) level on the enthalpies of formation, hydrogenation, and isomerization at 298 K ($\Delta_f H^{298}$, $\Delta_{hyd}H^{298}$, and $\Delta_{isom}H^{298}$) to determine the ground-state stability of [3]-radialene along with that of 29 related compounds. They discussed the enthalpic relationships among [3]-radialene, products of its total and partial hydrogenation, and a few of their many structural isomers. They studied on some simpler related compounds containing the cyclopropane or cyclopropene moiety and some isomers of the [3]-radialene sequential hydrogenation series to look into the enthalpies of isomerization upon going from the highly unstable [3]-radialene series to their stable isomers [48].

T. Höpfner et al showed that [4]radialene could be cyclopropanated to yield novel derivatives of [4]rotane [15]. They investigated the isomerization behavior of [6]radialenes and also the addition of divalent species (carbenes, epoxidation) to them [55].

Density functional theory (hybrid exchange– correlation functional B3LYP) was used to study the dimerization of metallacyclocumulenes to metal (Ti, Ni, Zr) substituted radialenes by D. Jemmis et al. These were compared to the dimerization of ethylene to cyclobutane. They discussed the nature of bonding in these metal substituted radialenes [56].

M. Iyoda et al reported an efficient route to the synthesis of highly fuorescent hexaaryl[3]radialenes using the oligomerization of ate-type copper carbenoids, followed by cyclization with hexamethylditin and Pd(PPh3)4; the structures of the [3]dendralene and hexaaryl[3]radialenes were determined by X-ray crystallographic analysis. They investigated a one-pot synthesis of radialenes by either cyclooligomerization of cumulenic double bonds [57].

Recently, K. Matsumoto et al reported the synthesis of hexaaryl[3]radialenes, electrochemical properties, and alkali metal reduction of hexakis(2- pyridyl)[3]radialene and hexakis(3- pyridyl) [3]radialene [58].

M. Tætteberg, P. Bakken et al described the determination of the molecular structure of hexamethyl-[6]radialene experimentally by the gas electron diffraction method and by theoretically ab initio calculations (HF/6-3 lG* and MP2/6-3 lG*) [59]

1.4. Application on CRC

1.4.1. Molecular electronics

Molecular electronics is defined as the use of single molecule based devices or single molecular wires to perform signal and information processing. It is an interdisciplinary field combining the efforts of biologists, chemists, physicists, mathematicians, life, biomedical, and computer scientists, and material, protein, and genetic engineers from all over the world. Many say that this pattern follows Moore's law, which states that with each year that passes, the size of the technological components exponentially decreases. Molecular electronics will play an important part in the future of technological components because limit to the size of current electronic systems is approaching [60].

The first advantage of electronics at a molecular level is the size of the entire electronic device. A device built from nanostructures would be a thousand times smaller than silicon based devices. If the same amount of space needed by a silicon based device is used by a molecular based device, the information process would be many times faster and more powerful, which presents a second benefit for the use of

molecular scale technology**.** A third advantage would be the decreased cost to produce electronicdevices. The manufacturing costs would be smaller due to the shear number of molecules existing in a relatively small chemical reaction. If the technology is available to construct stable and efficient molecular circuits needed from specific chemicals, this would mean in principle that there are billions and billions of electric connectors. [61]

It is necessary to comment on the fact that there are disadvantages to current nanoscale technology, but the chance of them being solved in the future is expected. One main disadvantage is that the processes of making connections to control, input, and output circuitry are difficult. This is because the circuitry is so small. Another disadvantage is that most molecules are generally thermally unstable. This means that they are capable of malfunctioning at high temperatures. However, some molecules do have a thermal stability higher than that of silicon. Third disadvantage is the lack of technology necessary to construct reliable and efficient nanoelectronicsystems.

Molecular electronics can be classified into Molecular Wires and Switches.

1.4.1.1. Molecular Wires

Molecular wires are made up of two parts: the molecules and two electrodes. A molecular wire must posses several different properties to be of any use. First, it must be able to conduct electrons along its length. This is completed by the movement of either a hole or electrons in electronic molecular wires and by excitation in a photonic wire as well as other types of electron movement on the molecular level. Second, the wire must also be easily oxidized or reduced. A third feature that a molecular wire must have is an insulating sheath to prevent the current from leaking to the surroundings. Finally, molecular wires must have a defined and fixed length [62].

Carbon-Rich structure–function relationships provide extremely useful guidance for the future rational design of molecules and polymers for nonlinear optical device applications. Monodisperse PTA oligomers serve as excellent models to provide specific information concerning the structural, electronic, and optical properties of their corresponding polydisperse long-chain polymeric analogs. A second interest in monodisperse π-conjugated oligomers of defined length and constitution arises from

their potential to act as molecular wires in molecular scale electronics and nanotechnological devices [63]

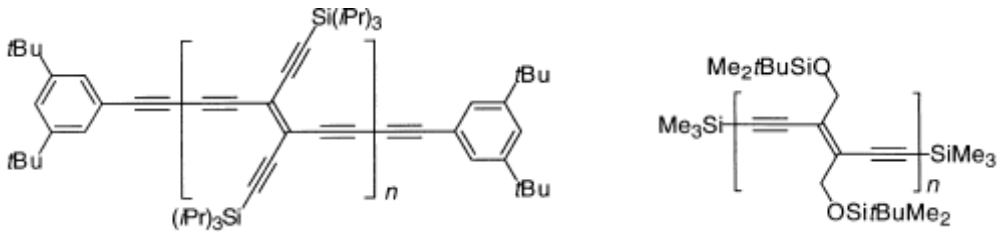

Figure 1.7. PTA oligomers can be used as molecular wires.

Thus, linear conjugation has been investigated in a series of monodisperse poly(triacetylene) rods extending in length up to 18 nm. It was found that saturation of electronic properties occurs at about 10 monomer units, corresponding to an effective conjugation length of about 60 C atoms.

1.4.1.2. Molecular Switches

Another device in molecular electronics is the switch. The definition of a molecular switch has changed from molecules being able to exist in two different thermodynamically states to having two different properties: being able to exist in two different states and to have an ON state (allowing a complete electron transfer to occur) and an OFF state (electron transfer is blocked) [64]. The switch processes can be,

(1) torsion process - twists the molecule around a single bond to achieve decoupling in the OFF state although no easy way has been discovered to twist and lock the molecule in place.

(2) saturation/unsaturation-a double bond is transformed into a single one therefore breaking conjugation. This is accomplished by reduction or molecular reorganization. ON and OFF states are obtained by deprotonation or protonation of the intervalence bands.

(3) quantum interfaces-based on electronic effects and uses the wave nature of electrons, and

(4) tunneling switch-works on excitation of the molecule.

Switches can be turned OFF by either changing the barrier height or the depth of the potential well. Switches are needed in all types of circuits where charge flow is needed at some time intervals and not at others. They may also be used for data registers at some point in the future, allowing for memory storage [65].

The development and investigation of the TEE chemistry and physics has greatly expanded the fundamental and technological perspectives of acetylenic nanoscaffolds. First waveguides based on molecular photoswitches was prepared in [47]. Arylated TEEs and DEEs are ideal components for molecular switches. They are able to undergo reversible, clean and rapid photochemical *cis* to *trans* and *trans* to *cis* isomerization, a property that is not exhibited by the nonarylated derivatives, without competing thermal isomerization pathways. Thereby these features pave the way for applications as light-driven molecular switches [65] in optoelectronic devices.

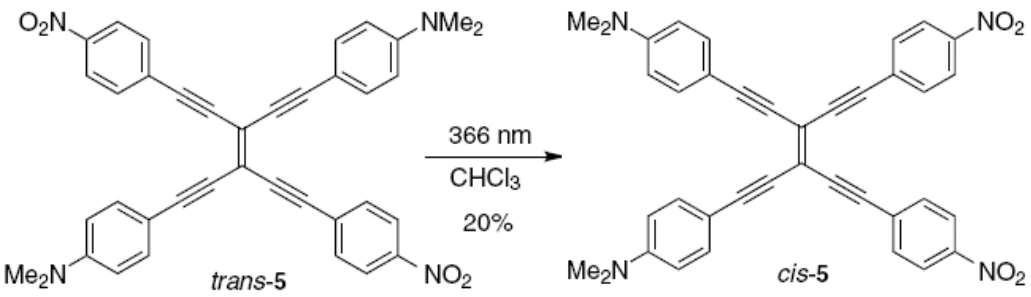

Figure 1.8. Photochemical trans – cis isomerization

By taking advantage of the proton-switchable strong luminescence of twisted intramolecular charge-transfer (TICT) states in *N,N*-dialkylaniline-substituted TEEs, multi-way chromophoric molecular switches were obtained. Thus, a sophisticated three-way chromophoric molecular switch was developed, which undergoes up to three switching processes under light and/or proton stimulus, leading up to eight different states most of which can be individually addressed. [66].

1.5. The Twisted Intramolecular Charge Transfer (TICT) Model

Lippert and co-workers first discovered dual fluorescence in organic donor - acceptor compounds in 1962 [68]. They reported the dual fluorescence of simple donor–acceptor substituted benzene derivative 4N,N-dimethylaminobenzonitrile (DMABN) with its normal band (B band at around 350 nm) is due to the initial excitation to the locally excited (LE) state and its anomalous one (A band, around 450 nm in medium polar solvent) is due to emission from an internal charge-transfer (CT) state. The two bands strongly depended on solvent polarity and temperature. In nonpolar solvents, only one fluorescence band appears, originating from the LE state. In polar solvents, a further long-wavelength fluorescence band grows in relative intensity, while the intensity of the first band decreases with increasing polarity of the medium [69].

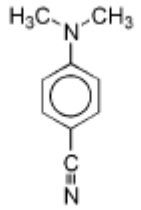

Figure 1.9. 4N,N-dimethylaminobenzonitrile (DMABN)

The Twisted Intramolecular Charge Transfer (TICT) was put forward by Grabowski and co-workers [70] to account for this observation.

The TICT model assumes that the molecule from its LE state relaxes to a minimum on the excited-state surface by twisting the donor group into a plane perpendicular to the acceptor group. Along this twisting coordinate, there is an increase of the charge transfer from the donor to the acceptor group, which leads to the highly polar structure responsible for the A-band emission. For the perpendicular TICT conformation donor (dialkylamino group) acceptor (benzonitrile) p-orbitals are ortogonal (zero overlap) and thus decoupled leading to a maximum for the dipole moment in the excited state and minimum in the ground state. The reaction processes summarized in Figure 1.10.

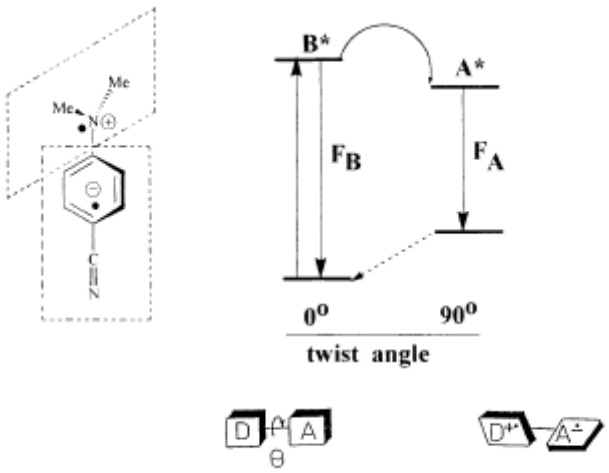

Figure 1.10. Representation of the TICT model for 4N,N-dimethylaminobenzonitrile (DMABN)

$$E_{LE} - E_{TICT} > 0 \qquad [1.1]$$

$$E_{TICT} = IP\,(D) - EA\,(A) + C + E_{solvent} \qquad [1.2]$$

Equations 1.1 and 1.2 can be used to predict possible new TICT systems [71]. The energetic minimum of the TICT state depends on the electron donor–acceptor property of the subsystems which can be quantified by ionization potential IP and affinity of donor D and acceptor A.

LE state responds less to changes in donor–acceptor property than TICT state. Polar solvent stabilization $E_{solvent}$ and Coulombic attraction C also help to stabilize the TICT state with respect the LE state. [73]

After the first general overview of the TICT concept [70], the rapidly growing volume of literature has been widely reviewed several times, with respect to both the diversity of the compounds displaying similar behavior and the physical phenomena involved. Much new evidence and several controversial hypotheses and quantum-chemical calculations have been reported with time [70,72].

The TICT phenomena were found in very different areas of pure and applied science. Along with well-substantiated papers, a lot of articles were published which attempted to assign very various findings to the TICT process. So far there is already a rich list of literature exceeding 1000 papers (prior to the beginning of the year 2002).

Applicational aspects are growing in various fields such as tailor-making of fluorescence probes [74], sensing of free volume in polymers [75, 76], fluorescent pH or ion indicators [77], fluorescent solar collectors, and electron transfer photochemistry for the destruction of harmful chlorinated aromatics [74].

The photophysical properties of N,N-dimethylaniline- (DMA) substituted TEE and related derivatives were investigated in both experimental and computational study. Measurements of the electronic emission spectra showed that these novel chromophores display a dual fluorescence, which strongly depends on solvent polarity. Their computational studies suggested that TICT model offers a possible explanation for the experimentally observed dual fluorescence. They used AM1 Method for the optimization of structures and TDDFT Method for excited state [78].

The aim of this study is to perform the chemical quantum calculations for acyclic and cyclic carbon reach compounds mentioned above. Ground state configurations, electronic structures, excited state energies and excited state behaviors and also compounds which show Twisted Intramolecular Charge Transfer (TICT) will be explored. In this thesis study, topics can be summarized below:

- comparison of electronic and spectroscopic properties of cyclic and acyclic TEE derivatives
- determination of the effects of increasing size of Radialenes and expanded Radialenes on the stability, energy difference of HOMO-LUMO, excited energies or wavelengths.
- The effect of acceptor strength on the TICT behavior

CHAPTER II

COMPUTATION ASPECT

2.1. Ground State Calculations

2.1.1 Ab initio methods

The term *ab initio* means from first principles. It does not mean that we are solving the Schrödinger equation exactly. It means that we are selecting a method that in principle with no inclusion of experimental data can lead to a reasonable approximation to the solution of the Schrödinger equation and then selecting a basis set that will implement that method in a reasonable way [79].

$$\hat{H}\,\mathbf{\Psi} = \mathrm{E}\,\mathbf{\Psi} \qquad [2.1]$$

The Hamiltonian is the total energy operator for a system, and is written as the sum of the kinetic energy of all the components of the system and the internal potential energy. Thus for the kinetic energy in a system of *M* nuclei and *N* electrons (atomic unit):

$$\hat{T}_N = -\sum_{\mathrm{A}}^{\mathrm{M}} \frac{1}{2\mathrm{M_A}} \nabla_{\mathrm{A}}^2 \qquad [2.2]$$

$$\hat{\mathrm{T}}_{\mathrm{e}} = -\sum_{i}^{N} \frac{1}{2} \nabla_i^2 \qquad [2.3]$$

And for the potential energy:

$$\hat{V}_{NN} = \sum_{A>B}^{M} \frac{Z_A Z_B}{r_{AB}} \qquad [2.4]$$

$$\hat{V}_{ee} = \sum_{i>j}^{N} \frac{1}{r_{ij}} \qquad [2.5]$$

$$\hat{V}_{eN} = -\sum_{A}^{M} \sum_{i}^{N} \frac{Z_A}{r_{iA}} \qquad [2.6]$$

Since, $\hat{H} = \hat{T} + \hat{V}$

$$\hat{H} = -\sum_{i}^{N} \frac{1}{2} \nabla_i^2 - \sum_{A}^{M} \sum_{i}^{N} \frac{Z_A}{r_{iA}} + \sum_{i>j}^{N} \frac{1}{r_{ij}} - \sum_{A}^{M} \frac{1}{2M_A} \nabla_A^2 + \sum_{A>B}^{M} \frac{Z_A Z_B}{r_{AB}} \qquad [2.7]$$

Within the Born-Oppenheimer (B-O) approximation [4], we assume the nuclei are held fixed while the electrons move really fast around them. (note: $M_p/M_e \approx 1840$.) In this case, nuclear motion and electronic motion are separated. The last two terms can be removed from the total hamiltonian to give the electronic hamiltonian, $\hat{H}_e$, since $\hat{V}_{NN} = K$, and $\nabla_A^2 = 0$. We will be working within the B-O approximation, so realizing

$$\hat{H}_e = -\sum_{i}^{N} \frac{1}{2} \nabla_i^2 - \sum_{A}^{M} \sum_{i}^{N} \frac{Z_A}{r_{iA}} + \sum_{i>j}^{N} \frac{1}{r_{ij}} \qquad [2.8]$$

We completely define the problem. Solving the electronic Schrödinger equation using this will give the electronic structure of a molecular system at a fixed nuclear geometry.

We know that the Schrödinger equation involving is intractable, so let's consider a simpler problem, involving the one-electron Hamiltonian

$$\hat{h}(i) = -\frac{1}{2} \nabla_i^2 + \sum_{A}^{M} \frac{1}{r_{iA}} \qquad [2.9]$$

which involves no electron-electron interaction. We construct a simpler system with Hamiltonian

$$\hat{H} = \sum_{\mathrm{i}}^{\mathrm{N}} \hat{h}(\mathrm{i}) . \qquad [2.10]$$

It will have eigenfunctions which are simple products of occupied spin orbitals (Orbital approximation), and thus an energy which is a sum of individual orbital energies, as

$$\Psi^{HP} = X_i(x_1)X_j(x_2)X_k(x_3)\cdots X_n(x_N) \qquad [2.11]$$

$$\langle \mathbf{\Psi} \left| \hat{H} \right| \mathbf{\Psi} \rangle = \varepsilon_{\mathrm{i}} + \varepsilon_{\mathrm{j}} + \varepsilon_{\mathrm{k}} \mathbf{...} \varepsilon_{\mathrm{n}} = \mathrm{E} . \qquad [2.12]$$

This kind of wavefunction is called a Hartree Product, and it suffers from several major flaws that serve to make them physically unrealistic. First, Hartree products do not satisfy the Pauli Antisymmetry Principle which states that the sign of any many-electron wave function must be antisymmetric (change sign) with respect to the interchange of the coordinates, both space and spin, of any two electrons. Second, Hartree products force a particular electron to occupy a given spin orbital despite the fact that electrons are indistinguishable from one another. Lastly, because the Hartree product wave function is constructed on the assumption that the electrons are non-interacting, there exists a non-zero probability of finding two electrons occupying the exact same point in space [80].

For our two electron problem, if we satisfy the antisymmetry principle, it can be obtained as a mathematical form of this wavefunction and generated by

$$\Psi = \frac{1}{\sqrt{N!}} \begin{vmatrix} \mathrm{X_i}(x_1) & \mathrm{X_j}(x_1) & \cdots & \mathrm{X_n}(x_1) \\ \mathrm{X_i}(x_2) & \mathrm{X_j}(x_2) & \cdots & \mathrm{X_n}(x_2) \\ \vdots & \vdots & \ddots & \vdots \\ \mathrm{X_i}(x_N) & \mathrm{X_j}(x_N) & \cdots & \mathrm{X_n}(x_N) \end{vmatrix} . \qquad [2.13]$$

A determinant of spin orbitals is called a Slater determinant. An interesting consequence of this functional form is that the electrons are all indistinguishable. Each electron is associated with every orbital!

Since we can always construct a determinant (within a sign) if we just know the list of the occupied orbitals $\{X_i(\mathrm{x}), X_j(\mathrm{x}), \ldots X_k(\mathrm{x})\}$, we can write it in shorthand in a ket symbol as $\left|X_i X_j \ldots X_k\right\rangle$ or even more simply as $\left|\mathrm{ij}\ldots\mathrm{k}\right\rangle$.

It is not at all obvious at this point, but it turns out that the assumption that the electrons can be described by an antisymmetrized product (Slater determinant) is equivalent to the assumption that each electron moves independently of all the others except that it feels the Coulomb repulsion due to the average positions of all electrons (and it also experiences a strange ``exchange'' interaction due to antisymmetrization). Hence, Hatree-Fock theory is also referred to as an *independent particle model* or a *mean field* theory [81].

Now that we know the functional form for the wavefunction in Hartree-Fock theory, we continue to simplify the problem by writing $\hat{H}_e$ as a sum of one- and two-electron operators.

$$\hat{H}_e = \sum_{\mathrm{i}} \hat{h}(\mathrm{i}) + \sum_{\mathrm{i>j}}^{\mathrm{N}} \frac{1}{\mathrm{r_{ij}}} \qquad [2.14]$$

$$= \hat{H}^{core} + \hat{H}_2 \,. \qquad [2.15]$$

The energy will be given by the usual quantum mechanical expression (assuming the wavefunction is normalized):

$$\mathrm{E_{el}} = \langle \boldsymbol{\Psi} \left| \hat{H}_{el} \right| \boldsymbol{\Psi} \rangle \qquad [2.16]$$

For symmetric energy expressions, we can employ the *variational theorem*, which states that the energy is always an upper bound to the true energy. Hence, we can obtain better approximate wavefunctions $\boldsymbol{\Psi}$ by varying their parameters until we minimize the energy within the given functional space. Hence, the correct molecular orbitals are those that minimize the electronic energy $\mathrm{E_{el}}$! The molecular orbitals can be

obtained numerically as a linear combination of a set of given basis functions (so-called "atomic orbital" basis functions, usually atom-cantered Gaussian type functions).

We can re-write the Hartree-Fock energy E_{HF} in terms of integrals of the one- and two-electron operators:

$$E_{HF} = \sum_{i} \langle i|h|i\rangle + \frac{1}{2}\sum_{ij}[ii \mid jj] - [ij \mid ji], \qquad [2.17]$$

where the one electron integral is

$$\langle i|h|j\rangle = \int dx_1 X_i^*(x_1) h(r_1) X_j(x_1) \qquad [2.18]$$

and a two-electron integral (Chemists' notation) is

$$[ij \mid kl] = \int dx_1 dx_2 X_i^*(x_1) X_j(x_1) \frac{1}{r_{12}} X_k^*(x_2) X_l(x_2) \qquad [2.19]$$

The Hartree-Fock method determines the set of spin orbitals, which minimize the energy and give us this ``best single determinant."

So, we need to minimize the Hartree-Fock energy expression with respect to changes in the orbitals $X_i \rightarrow X_i + \delta X_i$. We have also been assuming that the orbitals X are orthonormal, and we want to ensure that our variational procedure leaves them orthonormal. We can accomplish this by Lagrange's method of undetermined multipliers, where we employ a functional **L** defined as

$$L[\{X_i\}] = E_{HF}|\{X_i\}| - \sum_{ij} \varepsilon_{ij}(< i \mid j > -\delta_{ij}) \qquad [2.20]$$

Where ε_{ij} are the undetermined Lagrange multipliers and $< i \mid j >$ is the overlap between spin orbitals i and j,

$$< i \mid j >= \int X_i^*(\mathrm{x}) X_j(\mathrm{x}) d\mathrm{x} \qquad [2.21]$$

Setting the first variation $\delta \mathbf{L} = 0$, and working through some algebra, we eventually arrive at the Hartree-Fock equations defining the orbitals:

$$f(\mathrm{x}_1) X_i(\mathrm{x}_1) = \varepsilon_\mathrm{i} X_i(\mathrm{x}_1) \qquad [2.22]$$

and we can introduce a new operator, the *Fock operator*, as

$$f(\mathrm{x}_1) = h(\mathrm{x}_1) + \sum_j J_j(\mathrm{x}_1) - K_j(\mathrm{x}_1) \qquad [2.23]$$

First term is the one electron energy operator; second termis the classical coulomb repulsion of the electrons and third term is the exchange energy operator.

Introducing a basis set transforms the Hartree-Fock equations into the Roothaan equations. Denoting the atomic orbital basis functions as $\widetilde{X}$, we have the expansion

$$X_\mathrm{i} = \sum_{\mu=1}^{\mathrm{K}} \mathrm{C}_{\mu\mathrm{i}} \widetilde{X}_\mu \qquad [2.24]$$

for each spin orbital i. This leads to

$$f(\mathrm{x}_1) \sum_\upsilon \mathrm{C}_{\upsilon\mathrm{i}} \widetilde{X}_\upsilon(\mathrm{x}_1) = \varepsilon_\mathrm{i} \sum_\upsilon \mathrm{C}_{\upsilon\mathrm{i}} \widetilde{X}_\upsilon(\mathrm{x}_1) \qquad [2.25]$$

Left multiplying by $\widetilde{X}_\mu^*(\mathrm{x}_1)$ and integrating yields a matrix equation

$$\sum_\upsilon \mathrm{C}_{\upsilon\mathrm{i}} \int d\mathrm{x}_1 \widetilde{X}_\mu^*(\mathrm{x}_1) f(\mathrm{x}_1) \widetilde{X}_\upsilon(\mathrm{x}_1) = \varepsilon_\mathrm{i} \sum_\upsilon \mathrm{C}_{\upsilon\mathrm{i}} \int d\mathrm{x}_1 \widetilde{X}_\mu^*(\mathrm{x}_1) \widetilde{X}_\upsilon(\mathrm{x}_1) \qquad [2.26]$$

This can be simplified by introducing the matrix element notation

$$\mathbf{F}_{\mu\upsilon} = \int d\mathrm{x}_1 \widetilde{X}_\mu^*(\mathrm{x}_1) f(\mathrm{x}_1) \widetilde{X}_\upsilon(\mathrm{x}_1). \qquad [2.26]$$

$$= h_{uv} + \sum_{\mathrm{a}} \left[\sum_{\mathrm{p}\sigma} \mathrm{C}_{\mathrm{p}}^{\mathrm{a}} \mathrm{C}_{\sigma}^{\mathrm{a}} 2(uv \mid p\sigma) - (up \mid \sigma v) \right] \qquad [2.27]$$

$$= h_{uv} + \sum_{\mathrm{p}\sigma} \mathrm{D}_{\mathrm{p}\sigma} \left[2(uv \mid p\sigma) - (up \mid \sigma v) \right] \qquad [2.28]$$

and is the matrix representation of the Fock operator in the generic basis set. The quantity $\mathrm{D}_{\mathrm{p}\sigma}$ is known as either the density matrix or charge-density bond-order matrix because it recurs in the determination of these properties.

$$\mathbf{F}\,\mathrm{C} = \mathbf{S}\,\mathrm{C}\varepsilon \qquad [2.29]$$

$$\mathbf{S}_{\mu\upsilon} = \int d\mathrm{x}_1 \widetilde{X}_{\mu}^{*}(\mathrm{x}_1) \widetilde{X}_{\upsilon}(\mathrm{x}_1), \qquad [2.30]$$

Roothaan's basis set expansion method simplified the Hartree-Fock equations into a set of matrix equations comprised of matrix elements between basis functions and operators. The matrix elements are able to be evaluated using either analytical or numerical techniques, but Roothaan's method still has not solved one major problem: examination of the elements of the Fock matrix, reveals that the Fock operator depends on the very LCAO-MO coefficients one is trying to find, creating a difficult non-linear problem. The solution to this problem is to guess an initial form of the Fock matrix, typically the core Hamiltonian matrix h_{uv}, and generate an initial set of LCAO-MO coefficients using the process discussed at the tail end of section 1.8. From this initial set of coefficients one generates a better Fock matrix that can be used to get new coefficients and so on. This process is iterated until the LCAO-MO coefficients change by an amount less than some tolerance, i. e. until the system reaches self-consistency. The name given to this method is the self-consistent-field (SCF) method and it is one of the most important techniques in modern quantum chemistry [79].

2.1.2 Semiempirical Methods

As the system size increases, the problem become more difficult so it is necessary to be added approximations leading to Semiempirical Methods on Hartree-Fock Equation to simply solve [79].

Semiempirical Methods are simplified versions of Hartree-Fock theory using empirical corrections or having negligible values in order to improve performance. These methods are usually referred to through acronyms encoding some of the underlying theoretical assumptions. The most frequently used methods (MNDO, AM1, PM3) are all based on the Neglect of Differential Diatomic Overlap (NDDO) integral approximation, while older methods use simpler integral figures such as CNDO (Complete Neglect of Differential Overlap) assuming atomic orbitals to be spherical when evaluating the two-electron integrals and INDO (Intermediate Neglect of Differential Overlap) [82, 83].

All three approaches belong to the class of Zero Differential Overlap (ZDO) methods. This approximation simply says that the overlap between many atomic orbital will be small and thus the electron repulsion integrals will have negligible values

A number of additional approximations are made to speed up calculations and a number of parameterized corrections are made in order to correct for the approximate quantum mechanical model.

Originally, the initial semi-empirical methods (CNDO, INDO, and NDDO) only involved approximations to theoretical quantities. More recent methods (MNDO, AM1, and PM3) have involved the fitting of parameters to reproduce experimental data. AM1 and PM3 are generally considered to be an improvement over MNDO. For these methods the parameterization is performed such that the calculated energies are expressed as heats of formations instead of total energies [82].

In all these methods the core electrons (eg. the 1s electrons in C, O and N) are ignored as a further approximation.

The good side of semiempirical calculations is that they are much faster than the ab initio calculations.

The bad side of semiempirical calculations is If the molecule being computed is significantly different from anything in the parameterization set, the answers may be very poor.

Semiempirical calculations have been very successful in the description of organic chemistry, where there are only a few elements used extensively and the molecules are of moderate size.

2.1.3 Density Functional Theory

Hartree-Fock theory uses an exact Hamiltonian and approximates many - electron wavefunctions.

The correlations between electrons can be either long-range or short-range. Self-consistent field theory deals with long-range forces by using averaging techniques, i.e. the field experienced by an atom depends on the global distribution of the atoms. Short-range correlations, which involve the local environment around the atoms i.e. deviations, are not treated using the self-consistent field method. These short-range forces are often minor however in some cases, such as high temperature ceramic superconductors, these correlations are strong and need to be considered [80].

Kohn and Sham (1965) develop a theory to deal with this problem, this has been termed density functional theory since the electron density plays a crucial role. Effectively the energy is written as a function of the electron density rather than in terms of the many-electron wavefunctions. Approximations are made to the Hamiltonian [84].

Considering the forms of the energy for Hartree-Fock and for density functional theory can see the difference in the two techniques.

Hartree-Fock:

$$E_{HF} = \sum_{i=1}^{n} \varepsilon_i + \frac{1}{2}\sum_{i,j}^{n} J_{ij} - \frac{1}{2}\sum_{i,j}^{n} K_{ij} + V_{NN} \qquad [2.31]$$

Where V_{NN} is the nuclear repulsion energy, first term is the one electron (kinetic + potential) energy; second terms the classical coulomb repulsion of the electrons and third term is the exchange energy resulting from the quantum nature of the electrons.

Density functional theory:

$$E_{KS} = \sum_{i=1}^{n} \varepsilon_i + \frac{1}{2} \sum_{i,j}^{n} J_{ij} + E_X[n(r)] + E_C[n(r)] \qquad [2.32]$$

Where Ex[n(r)] is the exchange functional and E_C[n(r)] is the correlation potential. The exchange functional and correlation functionals are integrals of some function of the density and in some cases the density gradient.

For Hartree-Fock methods we know that The Hamiltonian is broken down into some basic one electron and two electron components as before, however the two electron components are further reduced to a combination of the Coulomb term and the exchanges correlation term(s). This extra term is incorporated into the Fock matrix. The correlation term is normally integrated numerically on a grid, or fitted to a Gaussian basis and then integrated analytically. The computationally intensive parts of the calculation involve the fitting of the density, the construction of the Coulomb potential, the construction of the exchange-correlation potential and the subsequent diagonalisation of the resulting equations.

The exchange correlation potential in density functional only the electron density determines theory, The precise dependence on density is not known except for the homogenous electron gas. For other situations the electron density varies through space and the assumption is made that the exchange correlation at a certain point is given by the homogeneous electron gas value involving the density at the same point. The charge density is determined and compared to the charge density used to generate the effective potential previously. If this is an improvement on the original charge density the cycle continues.

An initial guess is made to the electronic charge density, the Hartree potential and exchange correlation potentials are then calculated. The hamiltonian matrices for each of the k points included in the calculation are constructed and diagonalised to obtain the Kohn-Sham eigenstates. These eigenstates can then be used to generate the

charge density, a new set of Hamiltonian matrices is then generated and the process repeated until the output charge density is self-consistent with the charge density used to construct the electronic potentials.

In general, the Kohn-Sham equations are used rather than the Hartree-Fock equations, the methodology being very similar.

Note though that E_{KS} is *not* equal to the total energy of the system: The functionals are usually an integration over a function of the electron density and sometimes also its gradient, and it is this stage, because the 'exact' forms of these functionals are usually unknown, that introduces errors, because it becomes impossible to fully account for all many-body exchange and correlation properties. The various approximations to the exchange-correlation energy commonly used are necessary.

The most well known of which is probably the Becke-3- (B3) hybrid exchange functional usually used in combination with the Lee-Yang-Parr (LYP) correlation functional. The hybrid notation arises as HF exchange is mixed with the DFT definitions in defining the exchange-correlation term, examples of which are B3PW91 and B3LYP [85].

Density Functional Theory (DFT) has proved very successful in describing the static electronic structure of molecules of considerable size, including such properties as bonding energies, potential surfaces, geometries, vibrational structure and charge distributions in the past two decades.

2.2. Excited State Calculation

2.2.1. Time Dependent Density Functional Theory

In very many modern experiments physical properties are investigated by probing excitations. Since the last two decades a growing interest is observed especially in the optical spectroscopy methods. Although vast experimental data can be accessed, sadly, the theoretical understanding of the underlying physics is still far from being complete due to the lack of a good description of excited states. First attempts to study excited states via density-functional theory clearly indicated the limitations of this

method, which, so successful in case of the ground state, generally fails when blindly applied to excitations, and showed a need for overcoming this difficulty [79].

The method for calculating excited states using a time generalisation of DFT is called Time Dependent Density Functional Theory (TD-DFT). It is derived by applying a time dependent perturbation (e.g. light) to the ground state of a time independent system, modifying the external potential [86].

The time-dependent density of the interacting system of interest can be calculated as density

2.2.2. Configuration Interaction

An additional limitation of the HF method in general is that due to the use of the independent particle approximation the instantaneous correlation of the motions of electrons is neglected, even in the Hartree-Fock limit. The difference between the exact energy (determined by the Hamiltonian) and the HF energy is known as the *correlation* energy:

$$E_{correlation} = E_{exact} - E_{HF} < 0 \qquad [2.33]$$

There are several ways in which we can take into account the effects of instantaneous electron correlation, simply referred to as the correlation of the motions of electrons. One approach is to introduce the inter-electronic distances r_{ij} into the wavefunction. This method is only practical for systems with a few electrons. Another approach is configuration interaction.

Electrons repel each other, and prefer to be away from each other. The addition of excited configurations to the Hartree-Fock wave function, in which electrons have been excited from occupied to unoccupied spin orbitals, allows electrons to stay away from each other, thereby providing electron correlation. It gives a multi-determinant wave function. One approach to improving the Hartree-Fock wave function (Ψ_0) is to add a variationally determined amount of each of the excited configurations (Ψ_i) to the Hartree-Fock configuration. The resulting wave function is known as the full configuration interaction (Full CI) wave function (Ψ (Full CI))

$$\Psi_{(CI)} = a_0 \Psi_0 + \sum a_i \Psi_i \qquad [2.34]$$

The coefficient a_i is known as the amplitude of configuration Ψi .

For a given basis set of N basis functions, the full configuration interaction wave function and the corresponding full CI energy are the best possible. For a basis set of infinite size, the corresponding full CI wave function, containing an infinite number of configurations, gives the exact energy to the non-relativistic electronic Schrödinger equation. The full CI method is both variational and size consistent.

Although in practice we use basis sets of a finite size, even for moderately sized basis sets, the task of determining the full CI wave function is prohibitively large. Even with current supercomputers, it would take years possibly decades (if possible at all), to do a full CI calculation for even a simple system, e.g., $(NH_3)_2$. Thus, it is a practical necessity that electron correlation procedures attempt either to limit the number of configurations included, or to approximate the effect of their inclusion on the total wave function.

The most obvious approach to limiting the configurations included in the CI wave function, is to limit the levels of substitution included. The simplest way to supply is added single substitutions . This is termed Configuration Interaction, Singles (CIS).

$$\Psi_{CIS} = a_0 \Psi_0 + \sum_{i}^{occ} \sum_{a}^{virt} a_i^a \Psi_i^a \qquad [2.35]$$

Because of Brillouin's theorem, which states that single substitutions do not interact with the Hartree-Fock wave function, electron correlation is to include only double substitutions.

$$\Psi_{CID} = a_0 \Psi_0 + \sum_{i<j}^{occ} \sum_{i<j}^{occ} \sum_{a<b}^{virt} \sum_{a<b}^{virt} a_{ij}^{ab} \Psi_{ij}^{ab} \qquad [2.36]$$

At a slightly higher level of theory, single and double substitutions can be included in the configuration interaction treatment. This is termed Configuration Interaction, Singles and Doubles (CISD),

CHAPTER III

RESULTS

3.1 Radialenes and Expanded Radialenes

3.1.1 Ground state properties

It has been known that, DFT and semi-empirical calculations predict well the structures of carbon-rich acetylenic compounds [30], on the basis of this we have performed, our quantum chemical calculations at semiempirical and DFT level. AM1 method is used for semiempirical calculations, B3LYP functions and 3-21G*, 6-31G* basis sets are used in DFT calculations. TDDFT method is applied for the excited state calculations.

3.1.1.1 Radialenes

The calculations based on the AM1 and DFT/B3LYP/3-21G and 6-31G* basis sets for the ground state geometry optimization of radialenes and expanded radialenes for 3-6 ring size were carried out by using gaussian98 quantum chemical software package. DFT/B3LYP/6-31G* geometries and HOMO-LUMO structures are given in Figure 3.1, Figure 3.2, Figure 3.3, Figure 3.4, Figure 3.5, and Figure 3.6.Ground state energies of optimized structures for all radialenes and some of the geometric parameters which are endo and exo C-C bond lengths are listed in Tables 3.1. Although radialenes with size 3-5 have planar structures at all level of calculations, size 6 radialene has three dimensional chair structures like cyclo hexane. Also experimental results support the same conformation for these structures [47].

	a	**B**	**c**	**d**	e
2	–	–	–		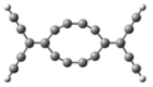
3	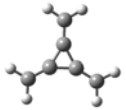	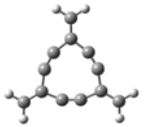	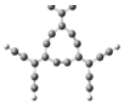	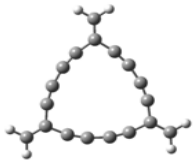	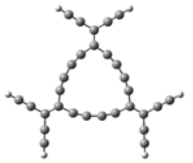
4	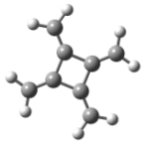	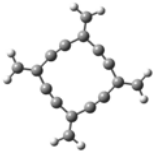	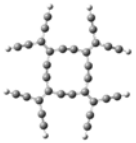	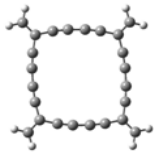	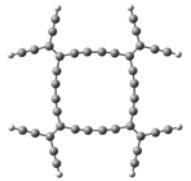
5	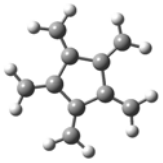	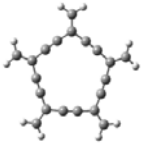		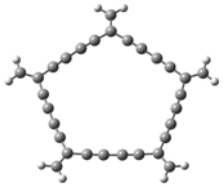	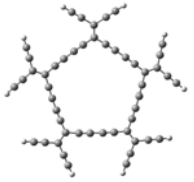
6	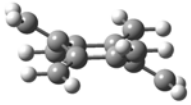	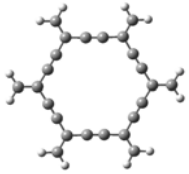		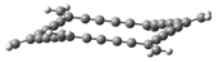	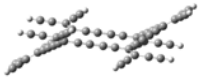

Figure 3.1. The DFT/B3LYP/6-31G* geometries of Radialenes and Expanded Radialenes

	2d	2e
L+2	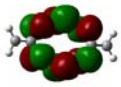	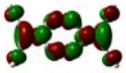
L+1	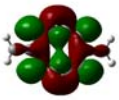	
L		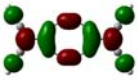
H		
H-1	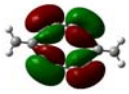	
H-2		

Figure 3.2. The structures of six frontier orbitals for radialenes and expanded radialenes with 2-size

	3a	3b	3c	3d	3e
L+2		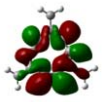	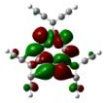		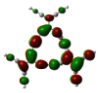
L+1		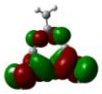	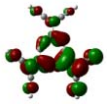		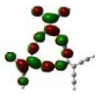
L			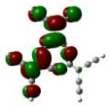		
H	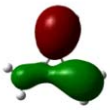		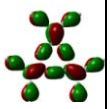		
H-1	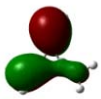				
H-2		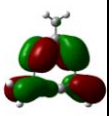		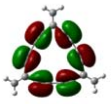	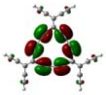

Figure 3.3. The structures of six frontier orbitals for radialenes and expanded radialenes with 3-size

	4a	4b	4c	4d	4e
L+2					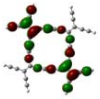
L+1					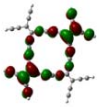
L					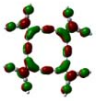
H					
H-1					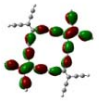
H-2					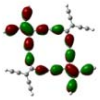

Figure 3.4. The structures of six frontier orbitals for radialenes and expanded radialenes with 4-size

	5a	5b	5c	5d	5e
L+2		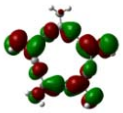		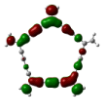	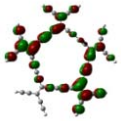
L+1	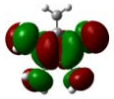	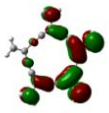			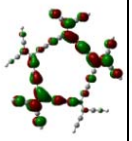
L		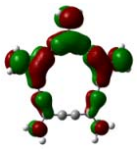	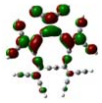		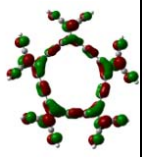
H			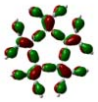		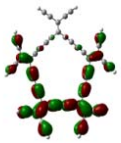
H-1	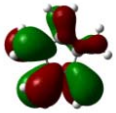	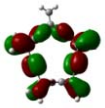	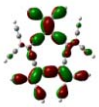		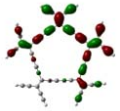
H-2		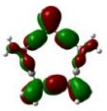	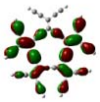	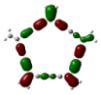	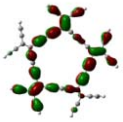

Figure 3.5. The structures of six frontier orbitals for radialenes and expanded radialenes with 5-size

	6a	6b	6c	6d	6e
L+2			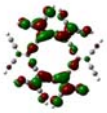		
L+1			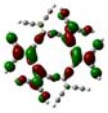	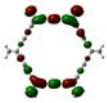	
L			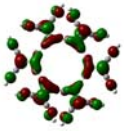		
H					
H-1			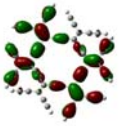	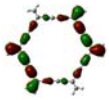	
H-2	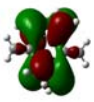	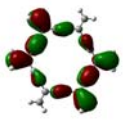			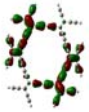

Figure 3.6 The structures of six frontier orbitals for radialenes and expanded radialenes with 6-size.

We observed the same trend in all three levels of calculations; there is no correlation between bond lengths and the size of radialenes. Endo C-C bond length of radialene[3] is shorter than the others around 0.05 Å. Endo C-C bond length of radialene[4] through radialene[6] which behave like an ordinary C-C single bond is varying between 1.47-1.49 Å at AM1 calculations, and 1.49-1.51 Å at DFT calculations. Also exo C-C bond length is 1.31-1.34 Å; nearly same for all radialenes and it is like a usual C-C double bond. Radialene[6] which has chair geometry, dihedral angle and the bond angle in the ring are 36 and 116 at AM1, 40 and 116 at DFT/3-21G*, and 38 and 116 at DFT/6-31G*. The similar values are obtained experimentally [35, 42].

Table 3.1. C-C bond lengths in Å for radialenes

AM1			**DFT-21G***			**DFT-631G***		
Subst.	**Endo sp^2-sp^2**	**Exo sp^2-sp^2**	**Subst.**	**Endo sp^2-sp^2**	**Exo sp^2-sp^2**	**Subst.**	**Endo sp^2-sp^2**	**Exo sp^2-sp^2**
3a	1.44	1.31	**3a**	1.46	1.33	**3a**	1.45	1.34
4a	1.49	1.32	**4a**	1.51	1.33	**4a**	1.50	1.34
5a	1.48	1.34	**5a**	1.50	1.33	**5a**	1.49	1.34
6a	1.47	1.34	**6a**	1.49	1.34	**6a**	1.49	1.34

The dihedral angle and bond angle in the ring for the chair geometry of rad[6] are 36° and 116° respectively according to AM1 results. The torsional angle is slightly bigger at the DFT level of calculations. The same angles in cyclo hexane are nearly 55° and 111°.

3.1.1.2 Expanded Radialenes:

In this part expanded radialenes with general formula $C_{4n}H_{2n}$, $C_{8n}H_{2n}$, $C_{6n}H_{2n}$ and $C_{10n}H_{2n}$ are investigated where n refers the number of edges in a polygon and takes the values 2,3,4,5, 6. The compound names that we gave and their general formulas are paired as 3b-6b; $C_{4n}H_{2n}$, 3c-6c; $C_{8n}H_{2n}$, 2d-6d; $C_{6n}H_{2n}$ and 2e-6e; $C_{10n}H_{2n}$. All of the

calculations show that all expanded radialenes with size 2 to 5 possess planar two dimensional structures and expanded radialene[6] usually has chair like structure.

a) $C_{4n}H_{2n}$: The endo (in the ring) sp^2-sp C-C bond length was found around 1.4 Å in all performed calculations and it falls between usual C-C single and double bond distance. Endo sp-sp bond length is about 1.2 Å, which is comparable to a C-C triple bond. Exo (outside the ring) sp2-sp^2 bond length is in between 1.3-1.4 Å. There is no big difference in calculations obtained by different methods. While AM1 method gives chair geometry for 6b(n=6) in which dihedral angle is 24°, angle in the ring is 117°, DFT calculations give planar geometry. As can be seen from Table 3.2, Table 3.3 and Table 3.4, the AM1 energy difference between chair and planar conformations is only 0.00008 au (0.002 eV).

Table 3.2. C-C bond lengths in Å of expanded radialenes with general formula $C_{4n}H_{2n}$ for AM1 method

Substance	**Endo sp-sp^2**	**Endo sp-sp**	**Exo sp^2-sp^2**
3b	1.42	1.20	1.34
4b	1.42	1.20	1.34
5b	1.41	1.19	1.35
6b	1.41	1.19	1.35

Table 3.3. C-C bond lengths in Å of expanded radialenes with general formula $C_{4n}H_{2n}$ for DFT/3-21G* calculations

Substance	Endo $sp\text{-}sp^2$	Endo sp-sp	Exo $sp^2\text{-}sp^2$
3b	1.44	1.21	1.34
4b	1.43	1.21	1.34
5b	1.43	1.21	1.35
6b	1.43	1.21	1.35

Table 3.4. C-C bond lengths in Å of expanded radialenes with general formula $C_{4n}H_{2n}$ for DFT/6-31G* calculations

Substance	Endo $sp\text{-}sp^2$	Endo sp-sp	Exo $sp^2\text{-}sp^2$
3b	1.44	1.22	1.35
4b	1.44	1.22	1.35
5b	1.43	1.21	1.35
6b	1.43	1.21	1.36

b) $C_{8n}H_{2n}$: For this kind of radialenes only AM1 and DFT/6-31g* calculations were performed. All of the compounds are planar except 6c which has a chair structure. We observe that the dihedral angle of 6c is bigger than 6b.

Table 3.5. C-C bond lengths in Å of expanded radialenes with general formula $C_{8n}H_{2n}$ for AM1 method

Substance	Endo $sp\text{-}sp^2$	Endo sp-sp	Exo $sp^2\text{-}sp^2$	Exo $sp\text{-}sp^2$	Exo sp-sp
3c	1.42	1.20	1.36	1.41	1.19
4c	1.42	1.20	1.37	1.41	1.19
5c	1.41	1.19	1.37	1.41	1.19
6c	1.41	1.20	1.37	1.41	1.19

Table 3.6. C-C bond lengths in Å of expanded radialenes with general formula $C_{8n}H_{2n}$ for DFT/3-21G* calculations

Substance	Endo $sp\text{-}sp^2$	Endo sp-sp	Exo $sp^2\text{-}sp^2$	Exo $sp\text{-}sp^2$	Exo sp-sp
3c	1.42	1.20	1.38	1.41	1.19
4c	1.42	1.20	1.38	1.42	1.19
5c	1.41	1.20	1.37	1.41	1.19
6c	1.42	1.20	1.39	1.42	1.20

Table 3.7. C-C bond lengths in Å of expanded radialenes with general formula $C_{8n}H_{2n}$ for DFT/6-31G* calculations

Substance	Endo sp-sp^2	Endo sp-sp	Exo sp^2-sp^2	Exo sp-sp^2	Exo sp-sp
3c	1.42	1.22	1.38	1.41	1.20
4c	1.41	1.20	1.37	1.41	1.19
5c	1.41	1.20	1.37	1.41	1.19
6c	1.42	1.22	1.39	1.42	1.20

c) $C_{6n}H_{2n}$: AM1 and DFT/6-31G* calculations provide chair structure similar to the previous compounds for radialene[6], however DFT/3-21G* geometry is planar. The energies of planar and chair conformations are very close to each other, which is about $5x10^{-5}$ au (0.00136 eV). The dihedral angle in AM1 results (34^o) is slightly bigger than DFT results (27^o) for 6d. As shown in Table 3.8, Table 3.9, and Table 3.10 that the bond lengths are so close to each others for different calculations, but in DFT results they are a bit longer.

Table 3.8. C-C bond lengths in Å of expanded radialenes with general formula $C_{6n}H_{2n}$ for AM1 method.

Substance	Endo sp-sp^2	Endo sp-sp	Endo sp-sp	Exo sp^2-sp^2
2d	1.43	1.21	1.35	1.34
3d	1.41	1.20	1.35	1.34
4d	1.40	1.20	1.35	1.35
5d	1.41	1.20	1.35	1.35
6d	1.41	1.20	1.35	1.35

Table 3.9. C-C bond lengths of in Å expanded radialenes with general formula $C_{6n}H_{2n}$ for DFT/3-21G* calculations

Substance	Endo $sp\text{-}sp^2$	Endo sp-sp	Endo sp-sp	Exo $sp^2\text{-}sp^2$
2d	1.44	1.22	1.36	1.35
3d	1.43	1.22	1.35	1.35
4d	1.43	1.21	1.35	1.35
5d	1.43	1.21	1.35	1.35
6d	1.43	1.21	1.35	1.36

Table 3.10. C-C bond lengths in Å of expanded radialenes with general formula $C_{6n}H_{2n}$ for DFT/6-31G* calculations

Substance	Endo $sp\text{-}sp^2$	Endo sp-sp	Endo sp-sp	Exo $sp^2\text{-}sp^2$
2d	1.45	1.23	1.37	1.35
3d	1.43	1.22	1.36	1.35
4d	1.43	1.22	1.36	1.35
5d	1.43	1.22	1.36	1.36
6d	1.42	1.22	1.36	1.36

d) $C_{10n}H_{2n}$: All the methods give three dimensional chair structures for 6e compared to the former compounds**,** and the dihedral angle is 22-23^o at DFT level, and is 41 at AM1 level of calculations. The energy difference with planar one is again on the order of 0.001 eV.

Table 3.11. C-C bond lengths in Å of expanded radialenes with general formula $C_{10n}H_{2n}$ for AM1 method.

Substance	Endo $sp\text{-}sp^2$	Endo sp-sp	Endo sp-sp	Exo $sp^2\text{-}sp^2$	Exo $sp\text{-}sp^2$	Exo sp-sp
2e	1.42	1.21	1.35	1.36	1.41	1.19
3e	1.41	1.20	1.35	1.37	1.41	1.19
4e	1.41	1.20	1.35	1.37	1.41	1.19
5e	1.41	1.20	1.35	1.37	1.41	1.19
6e	1.41	1.20	1.35	1.38	1.41	1.19

Table 3.12. C-C bond lengths in Å of expanded radialenes with general formula $C_{10n}H_{2n}$ for DFT/3-21G* calculations

Substance	Endo $sp\text{-}sp^2$	Endo sp-sp	Endo sp-sp	Exo $sp^2\text{-}sp^2$	Exo $sp\text{-}sp^2$	Exo sp-sp
2e	1.43	1.23	1.35	1.38	1.41	1.20
3e	1.42	1.22	1.35	1.39	1.41	1.20
4e	1.42	1.22	1.35	1.39	1.41	1.20
5e	1.41	1.22	1.35	1.39	1.41	1.20
6e	1.42	1.22	1.34	1.39	1.41	1.20

Table 3.13. C-C bond lengths in Å of expanded radialenes with general formula $C_{10n}H_{2n}$ for DFT/6-31G* calculations

Substance	Endo $sp-sp^2$	Endo sp-sp	Endo sp-sp	Exo sp^2-sp^2	Exo $sp-sp^2$	Exo sp-sp
2e	1.43	1.23	1.36	1.39	1.42	1.21
3e	1.42	1.23	1.35	1.39	1.42	1.21
4e	1.42	1.22	1.35	1.39	1.42	1.21
5e	1.41	1.22	1.35	1.39	1.42	1.21
6e	1.41	1.22	1.35	1.40	1.42	1.21

3.1.2 Excited state properties

TDDFT/3-21G, TDDFT/6-31G* level of calculations are done for the excited state behaviors on AM1, DFT/3-21G* and DFT/6-31G*ground state structures. The notation like a TDDFT/3-21G//AM1, which we used below means that, TDDFT calculation is performed by using 3-21G-basis, set on AM1 geometry.

3.1.2.1 Radialenes

The shapes of six frontier orbitals, which include two orbital below Highest Occupied Molecular Orbital (H) through two orbitals above Lowest Unoccupied Molecular Orbital (L), are given in Figure 3.2, Figure 3.3, Figure 3.4, Figure 3.5, and Figure 3.6. As can be seen from this figure, H has π character on all double and triple bonds whereas L has π^* character for all types of radialenes.

Table 3.14 The first excited state properties of radialenes for TDDFT/6-31G*//DFT /6-31G* calculations.

Substance	ExE(s1)eV	λ_{max}	osc.st	dipole(s0)	dipole(s1)
3a	4.798	258	0.319	0.00	4.04
4a	3.884	319	0.000	0.00	0.00
5a	3.496	355	0.000	0.00	6.97
6a	3.947	314	0.038	0.00	0.00

The transition wavelength to the first excited state increases from 3a to 5a but in 6a it is less than 20-40 nm compared to 5a (Table 3.14). The reason of that, 6a has three dimensional structure, so that its two dimensional cross conjugation break down. Maximum wavelength increases with growing size of radialene for planar conformations.

Although ground state dipole moment is zero for all of them, excited state dipoles differ from zero for odd size Radialenes. Oscillator strength is zero for the first transitions except 3a and 6a. The H to L contribution to this transition is greatest for all radialenes. The transitions which have non-zero oscillator strength are doublet including one or several of the excitation to the 2;3, 7;8 9;10 excited states. Their transition nature and their contributions are summarized is given in Table 3.15 for the TDDFT/6-31G*//DFT/6-31G* calculations. The same trend is observed all of the methods that we used. Wavelengths obtained from TDDFT/6-31G*//DFT /6-31G* calculations are larger compared to the results obtained by the other methods. Our results agree with the electronic absorptions of radialenes in which were observed at 289- 208, 296, and 220 nm for 3a, 4a and 5a respectively [42].

Table 3.15. The transition natures which have non-zero oscillator strength, and their contributions for TDDFT/6-31G*//DFT/6-31G* calculations of radialenes and expanded Radialenes

Sub.	lamda	osc.st	state(nature,contribution)	lamda	osc.st	state(nature,contribution)
3a						
4a	254	0.132	S2(H-1;L,0.6),S3(H-2;L,0.6)	190	0.640	S7(H;L+1),S8(H;L+2)
5a	212	0.640	S7(H-2;L,0.4),s8(H-3;L,0.4)			
6a	230	0.008	S7(H-3;L,0.6),s8(H-4;L,0.6)	214	0.297	S9(H-1;L+1, H-2;L+2,0.4)
						S10(H-1;L+2, H-2;L+1,0.4)
3b	264	0.364	S10(H-1;L,0.36), (H-2;L+1,0.36)			
4b	320	0.069	S3(H-1;L,0.59),S4(H-2;L,0.59)	275	0.652	S10(H;L+1,0.47) 4tr
5b	316	0.291	S3(H-2;L,0.46),(H-1;L+1,0.46)			
			S4(H-2;L+1,0.46),(H-1;L,0.46)			
6b						
3c	379	0.760	S4(H-2;L,L+1,0.3),S5(H-1;L,L+1,0.3)			
	466	0.105	S2(H-1;L,0.52),S3(H-2,L,0.52)	381	1.257	S7(H;L+1,0.49),S8(H;L+2,0.49)
4c	476	0.475	S3(H-2;L,0.41,H-1;L+1,0.41)			
5c			S4(H-2;L+1,041,H-1;L,0.41)	383	0.370	S7(H;L+2,0.61),S8(H;L+3,0.61)
6c	480	0.378	S7(H-2;L+2,H-1;L+1,0.4)	454	0.186	S9(H-2;L+1,0.37,H-2;L+2,0.23)
			S8(H-2;L+1,H-1;L+2,0.4)			
2d	347	0.395	S5(H;L,0.56)	266	0.277	S10(H-3;L+1,0.54)
3d	368	0.211	S4(H;L,0.62),S5(H-1;L, 0.62)			
4d	365	0.100	S3(H-1;L,0.61),S4(H-2;L,0.61)	339	0.493	S9(H;L+1,0.57),S10(H;L+2,0.57)
5d	354	0.015	S6(H-2;L,0.44),S7(H-3;L,0.44)			
6d						
2e	489	1.184	S3(H;L,0.56)			
3e	402	0.675	S10(H-1,L+2,H;L+1,0.4)			
4e	542	0.091	S2(H-1;L,0.58),S3(H-2;L,0.58)	465	1.135	S7(H;L+1,0.51),S8(H;L+2)
5e	526	0.091	S3(H-2;L,0.4,H-1;L+1,0.38,H;L+2,0.38)	485	1.398	S7(H-2;L,0.41),S8(H-3;L,0.41)
			S4(H-3;L,0.4,H-1;L+2,0.38,H;L+1,0.38)			
6e						

3.1.2.2 Expanded Radialenes

a) $C_{4n}H_{2n}$ (3b-6b): Although maximum wavelength increases with the ring size for these class of compounds, the amount of increase is not linear as seen in Table 3.16. Oscillator strength is almost zero for all of them and again H-L transitions are dominant. The transitions where Oscillator strength different than zero are shown in Table 3.15. The wavelength of those transitions ranges from 260 to 320 nm and they differ from λ_{max} about 35-70 nm. In general, six frontier orbitals shown in Figure 3.2, Figure 3.3, Figure 3.4, Figure 3.5, and Figure 3.6 are used for these transitions. The excited state

dipole moments are non-zero for odd numbered ones as in the case of radialenes. (9.15. D)

Table 3.16. The first excited state properties of expanded radialenes with general formula $C_{4n}C_{2n}$ for TDDFT/6-31G*//DFT /6-31G* calculations.

Substance	ExE(s1)eV	λ_{max}	osc.st	dipole(s0)	dipole(s1)
3b	4.018	309	0.080	0.00	9.02
4b	3.652	339	0.000	0.00	0.00
5b	3.540	350	0.000	0.00	14.82
6b	3.461	358	0.000	0.00	0.00

b) $C_{8n}H_{2n}$(3c-6c): In these compounds ethylene groups are attached instead of hydrogens in the previous type of expanded radialenes. This change has great effect on the λ_{max} values, which shift bathochromically, about 150-200 nm to the VIS region. This can be explained by increasing cross conjugation length. The λ_{max} values are in range of 466-582 nm (Table 3.17). The transition to the first excited state is forbidden except rad[3]. The allowed transitions occur to the higher states and they are in the 360-480 nm and they still in the VISIBLE region.

Table 3.17. The first excited state properties of expanded radialenes with general formula $C_{8n}H_{2n}$ for TDDFT/6-31G*//DFT /6-31G* calculations.

Substance	ExE(s1)eV	λ_{max}	osc.st
3c	2.566	483	0.240
4c	2.397	517	0.000
5c	2.244	553	0.000
6c	2.131	582	0.036

c) $C_{6n}H_{2n}$(2d-6d): The λ_{max} values decrease as these class radialenes size increases according to TDDFT/6-31G*//6-31G* results. Whereas, we did not observe any correlation between λ_{max} and ring size for the other calculations. 2d has the largest

wavelength, and it is about 433-461 nm. The maximum wavelength change only about 20 nm in 3d-6d compounds except TDDFT/6-31G-//6-31G* results. When we growth the ring size with the addition of one more ethynyl groups compared to $C_{4n}H_{2n}$ radialenes λ_{max} values have red-shift about 100-150 nm. The transitions to the first excited state are not allowed for all size and most of them do not contain H-L nature. The transitions with non-zero transition dipole are observed between 347-368 nm. Excited state dipole is larger than zero only for n=5 and it has a large value.

Table 3.18. The first excited state properties of expanded radialenes with general formula $C_{6n}H_{2n}$ for TDDFT/6-31G*//DFT /6-31G* calculations.

Substance	ExE(s1)eV	λ_{max}	osc.st	dipole(s0)	dipole(s1)
2d	2.684	462	0.000	0.00	0.00
3d	2.936	422	0.000	0.00	0.01
4d	3.127	396	0.000	0.00	0.00
5d	3.233	383	0.000	0.00	20.81
6d	3.253	381	0.010	0.00	0.00

d) **$C_{10n}H_{2n}$(2e-6e):** The same effect is observed with the addition of ethynyl units outside the ring as in $C_{8n}H_{2n}$. The fluctuations in λ_{max}'s are not too much for different sizes. Only 3e has allowed transition to first excited state. Its nature is H to L and H-1 to L doublet. Wavelength is in between 490-597 nm. Again, the excited state dipoles of odd-size compounds are non-zero. For some transitions oscillator strength is greater than one that indicates very intense transitions. As can be seen from Table 3.15 these large peaks are in the visible region. H-L nature is dominant only for 2e.

Table 3.19. The first excited state properties of expanded radialenes with general formula $C_{10n}H_{2n}$ for TDDFT/6-31G*//DFT /6-31G* calculations.

Substance	ExE(s1)eV	λ_{max}	osc.st	dipole(s0)	dipole(s1)
2e	2.075	597	0.000	0.00	0.00
3e	2.303	538	0.446	0.00	13.05
4e	2.139	580	0.000	0.00	0.00
5e	2.091	593	0.000	0.00	24.04
6e					

3.2 TEE Monomer and Dimer

3.2.1 TEE Monomer

AM1 level of calculations are performed for all TEE monomers and dimers Ground State Behavior

3.2.1.1 Ground State Behavior

The effect of strength of the acceptor group on the push-pull chromophoric TEE derivatives is studied by the substitution of various acceptors such that p-NO_2-benzene- (T1), p-CHO-benzene- (T2), p-CH_3-benzene- (T3) on the excited and ground state behaviours. The donor-acceptor compounds that we worked on are given in figure 3.7, figure 3.8, and figure 3.9. The acceptor strengths increase in the order of p-NO_2-benzene- > p-CHO-benzene- > p-CH_3-benzene- according to Hammet and pK_a constants [87]. The region effect is also examined by attaching acceptor unit on

different location, which are mainly CIS, TRANS and GEMINAL with respect to donor positions at TEE. The structural parameters are given in Table 3.21.

The ground state energies are given in Table 3.20. All isomers of each acceptor units are close to each other energetically.

Table 3.20. The ground state energies of TEE derivatives with different positions of p-NO_2-benzene- , p-CHO-benzene-, p-CH_3-benzene-

Substance	AM1/au	Substance	AM1/au	Substance	AM1/au
CIS	0.4586834	CIS	0.404373	CIS	0.440987
TRANS	0.4590255	TRANS	0.404207	TRANS	0.440778
GEMINAL	0.4592191	GEMINAL	0.404826	GEMINAL	0.440842

In all substances, the bond length on centre of ethene part of the compounds is 1.37 Å which is larger than a usual double bond. That leads an easy rotation around this bond as predicted before by A. Hilger for the other TEE derivatives [30]. All the presumed single bonds and triple bonds on the all TEE derivatives worked on are 1.4 Å and 1.2 Å respectively.

The structural parameters for the donor group dimethylanilino (DMA) are not affected by the location of nitro group.

In trans p-CHO-benzene substituted TEEs, H_3C-N-CH_3 angle is slightly longer and pyramidal angle slightly shorter than cis and geminal isomers. However, in cis CH_3 substituted ones almost opposite of this situation are observed.

All TEE derivatives that we have studied are planar except cis-isomer. In cisT1, cisT2 and cisT3, the functional D/A groups are twisted about 8-10° from the TEE molecular plane. We also observed a 5° deviation from planarity on the TEE moiety for cisT1.

These observations show, as the acceptor group gets weaker sp^3 character of donor increases in CIS location. Trans position is not affected by the strength of donor. When the acceptor is placed at the GEM position for nitro and CH_3 acceptors the angle (C-N-C) is 117°, but in CHO it is 114°. We could not explain this at this stage.

Table 3.21. The structural parameters of TEE derivatives with different positions of p-NO_2-benzene-, p-CHO-benzene-, p-CH_3-benzene-

Substance	**Center sp^2-sp^2 double**	**C-C sp-sp^2 single**	**N-C sp^3-sp^2 single**	**C-N-C angle**	**Pyramidal dihedral angle**
cisT1	1.37	1.40	1.40	117	18
transT1	1.37	1.40	1.40	117	17
gemT1	1.37	1.40	1.40	117	18
Substance	**Center sp^2-sp^2 double**	**C-C sp-sp^2 single**	**N-C sp^3-sp^2 single**	**C-N-C angle**	**Pyramidal dihedral angle**
cisT2	1.37	1.40	1.41	114	26
transT2	1.37	1.40	1.40	117	19
gemT2	1.37	1.40	1.41	114	23
Substance	**Center sp^2-sp^2 double**	**C-C sp-sp^2 single**	N-C **sp^3-sp^2 single**	**C-N-C angle**	**Pyramidal dihedral angle**
cisT3	1.37	1.40	1.41	114	24
transT3	1.37	1.40	1.40	117	19
gemT3	1.37	1.40	1.40	117	19

Structure	HOMO	LUMO
CisT1 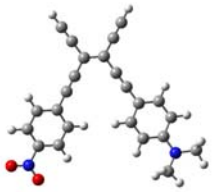	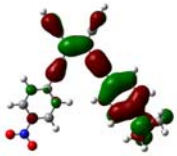	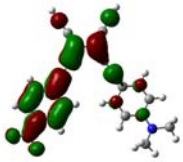
GemT1 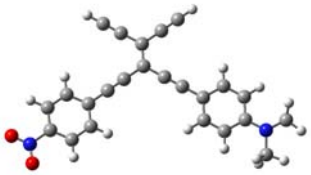	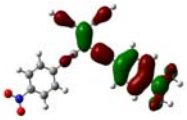	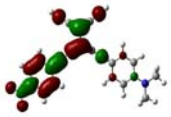
TransT1 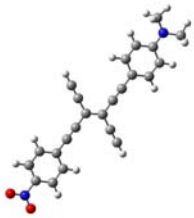	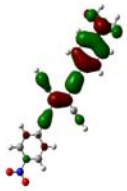	

Figure 3.7. HOMO-LUMO structures for all isomers of TEE derivative with p-NO_2-benzene-

Structure	HOMO	LUMO
cis 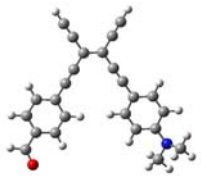	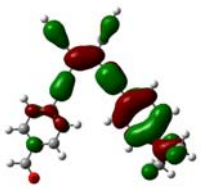	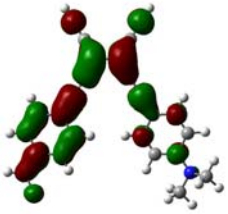
gem 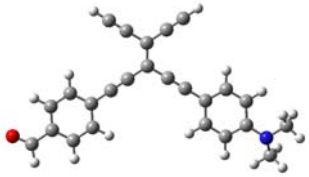	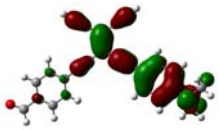	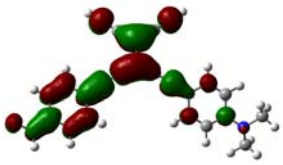
trans 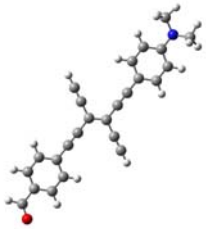	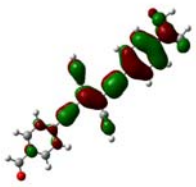	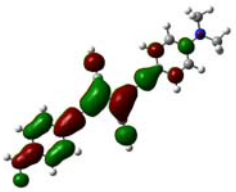

Figure 3.8. HOMO-LUMO structures for all isomers of TEE derivative with p-CHO-benzene-

Structure	HOMO	LUMO
cis 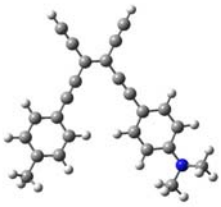	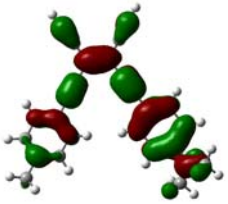	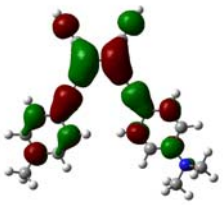
gem 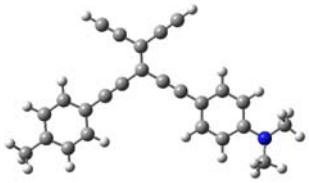	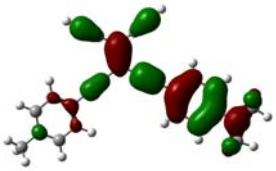	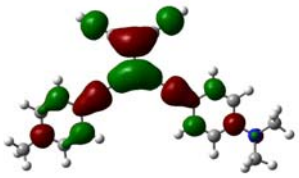
trans 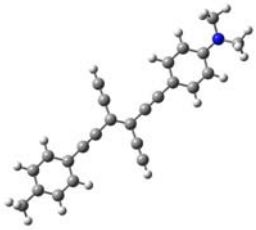	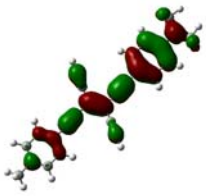	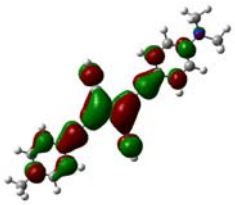

Figure 3.9. HOMO-LUMO structures for all isomers of TEE derivative with p-CH_3-benzene-

3.2.1.2 Excited State Behavior

3.2.1.2.1 Absorption:

Effect of acceptor strength:

Vertical transition frequencies and oscillator strengths are shown in Tables 3.22 for Tee derivatives as mentioned in previous section. A bathocromic shift is observed in all isomers when the acceptor unit is weakens. HOMO-LUMO shapes indicate that all p-NO_2-benzene- and p-CHO-benzene- moieties behave as acceptors in all related compounds. On the other hand, only benzene unit in which CH_3 is connected acts like an electron acceptor in Gem isomers. In cis and trans positions, CH_3 unit or benzene close to it, neither behaves like an acceptor nor donor, the electron migration occurs from DMA to the TEE part.

Table 3.22. Vertical transition frequencies and oscillator strengths of TEE derivatives with different position p-NO_2-benzene-, p-CHO-benzene-, p-CH_3-benzene-

	NO2/T1		**CHO/T2**		**CH_3/T3**	
	lamda(nm)	**osc.st**	**lamda(nm)**	**osc.st**	**lamda(nm)**	**osc.st**
CIS	512	0.42	491	0.45	444	0.64
GEM	505	0.21	475	0.27	462	0.58
TRANS	492	1.16	480	1.26	444	1.32

Although the wavelength difference between NO_2 and CH_3 derivatives about 70-75 nm for Cis and Gem isomers, it is about 50 nm for Trans isomer (See Table 3.22). This can be explained by examining the paths of electron flow. HOMO-LUMO figures

(Figure 3.7, figure 3.8, and figure 3.9) exhibit that trans isomer has linear conjugation path but gem and cis isomers have cross and two-dimensional conjugations path.

Effect of isomer:

Although trans isomer has lowest λ_{max}, cis isomer has largest but the difference is less than 20 nm in derivatives with NO_2. For the other derivatives cis isomer has largest and gem has the lowest λmax values. Then again it only differ about 20 nm. Cis and trans isomers have the same λ_{max} in compounds with CH_3. The electron density is constant in HOMO and LUMO in methyl units. Methyl unit is always electron deficient without regarding of its position for both HOMO and LUMO. As we mentioned in former section, in gem location electron migration is observed to the benzene ring near to CH_3, which may explain why λ_{max} of gemT3 is differ.

3.2.1.2.2 TICT:

The TICT behaviours of TEE derivatives, the effect of acceptor strength and their positions to TICT state are investigated by excited state calculations on AM1 geometries. The probable donor units on the TEE derivates are considered as dimethyl amine and DMA (dimethylamilino). Those units are rotated by the increments of 15º from the ground state structures without changing the rest of geometrical parameters in excited state calculations. We did not perform optimization for the rotated structure. In figures 3.10-3.18 ground and excited state energies, oscillator strengths, ground and excited state dipole moments are given as a function of rotation angle.

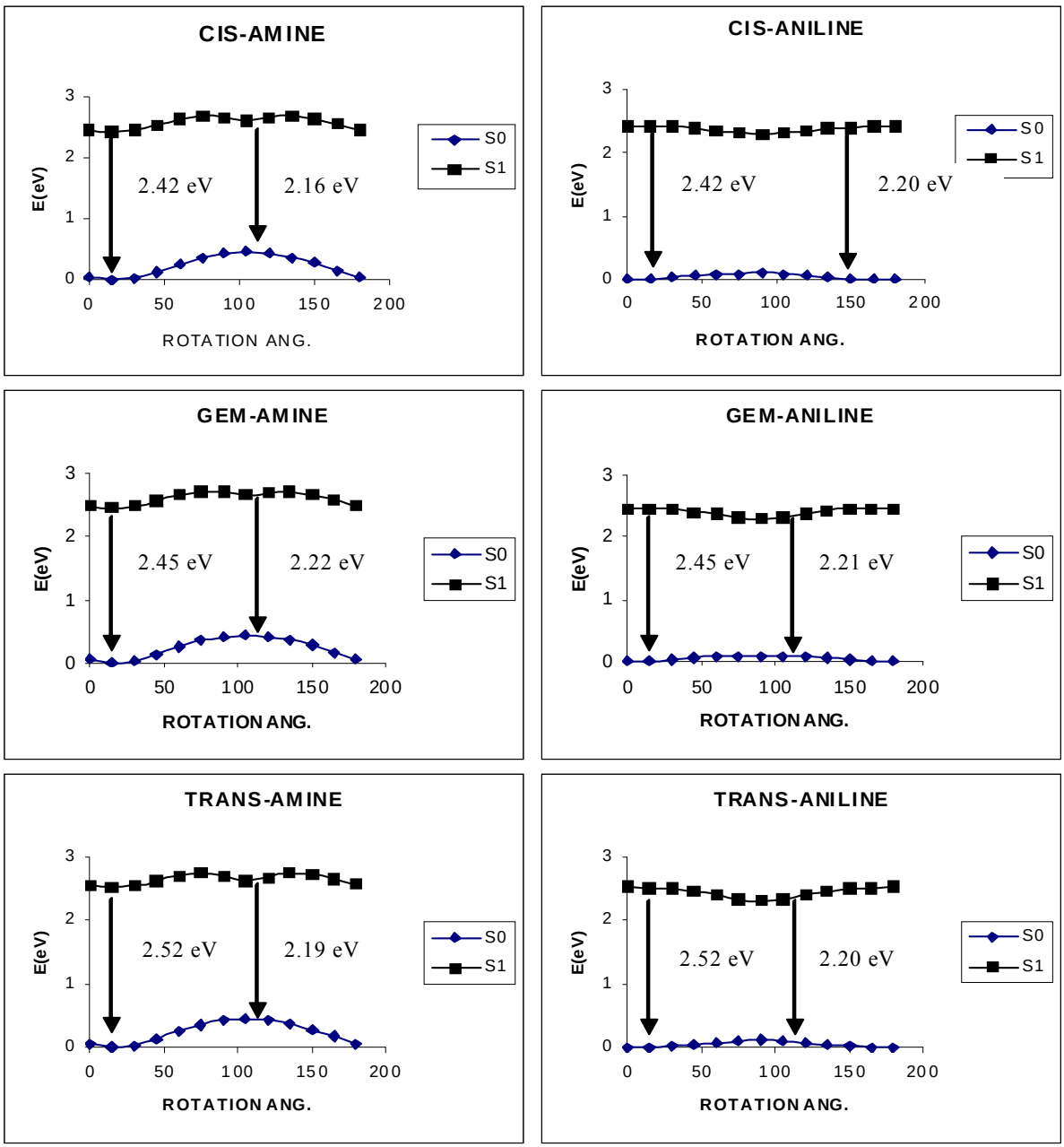

Figure 3.10. Ground and 1st excited state energies given as a function of rotation angle for all isomers of TEE derivative with NO_2

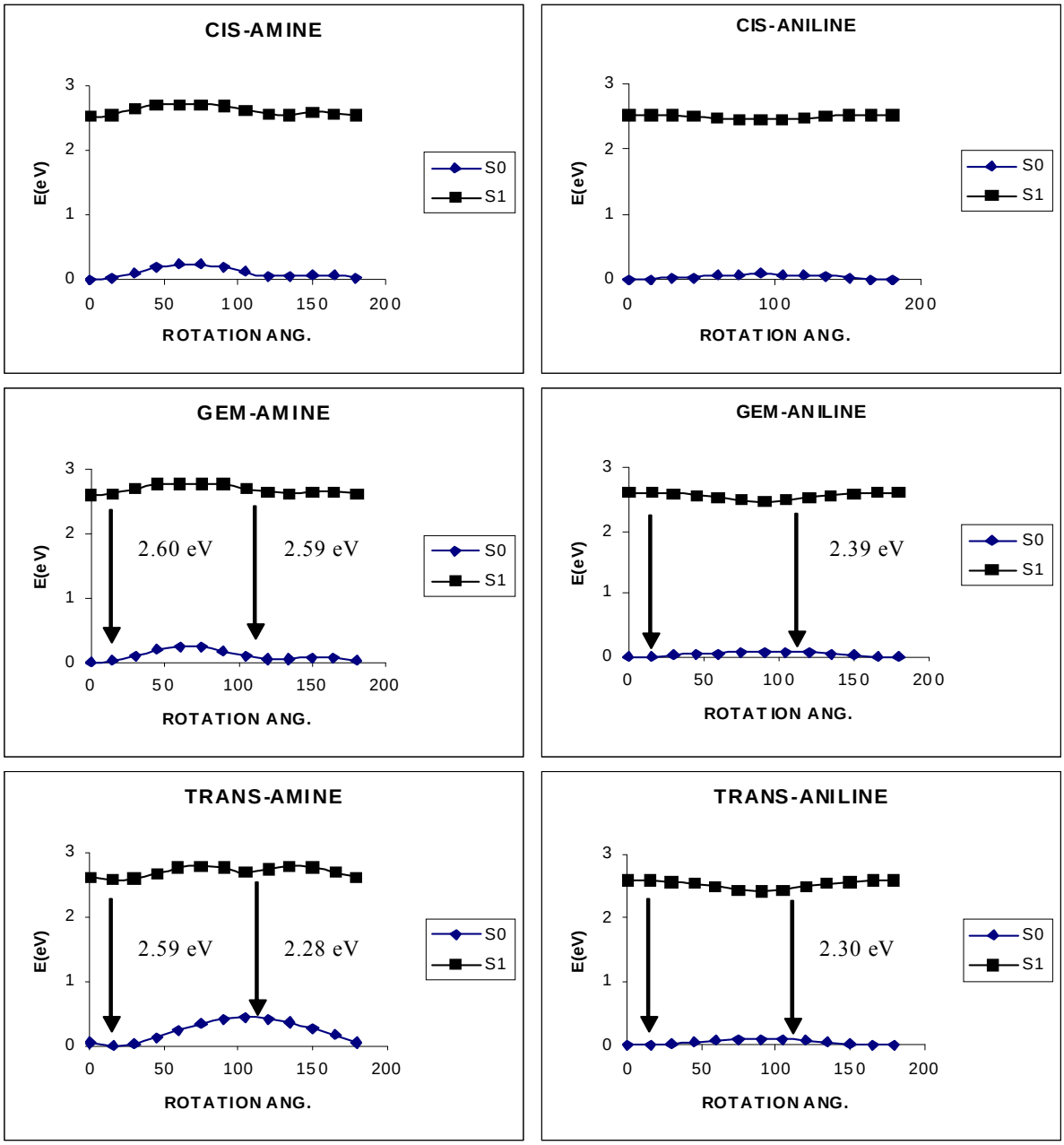

Figure 3.11. Ground and excited state energies given as a function of rotation angle for all isomers of TEE derivative with CHO

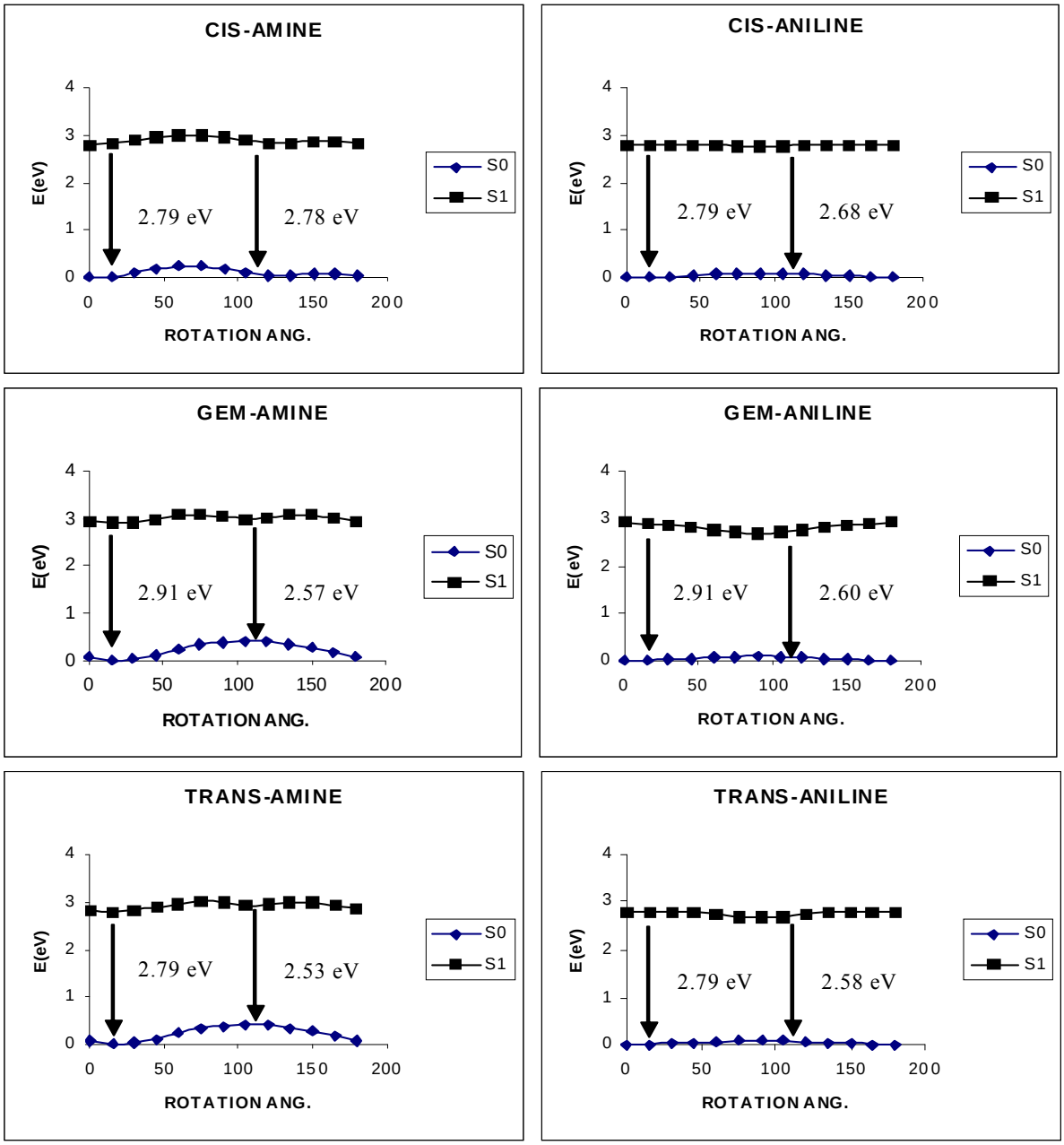

Figure 3.12. Ground and excited state energies given as a function of rotation angle for all isomers of TEE derivative with CH_3

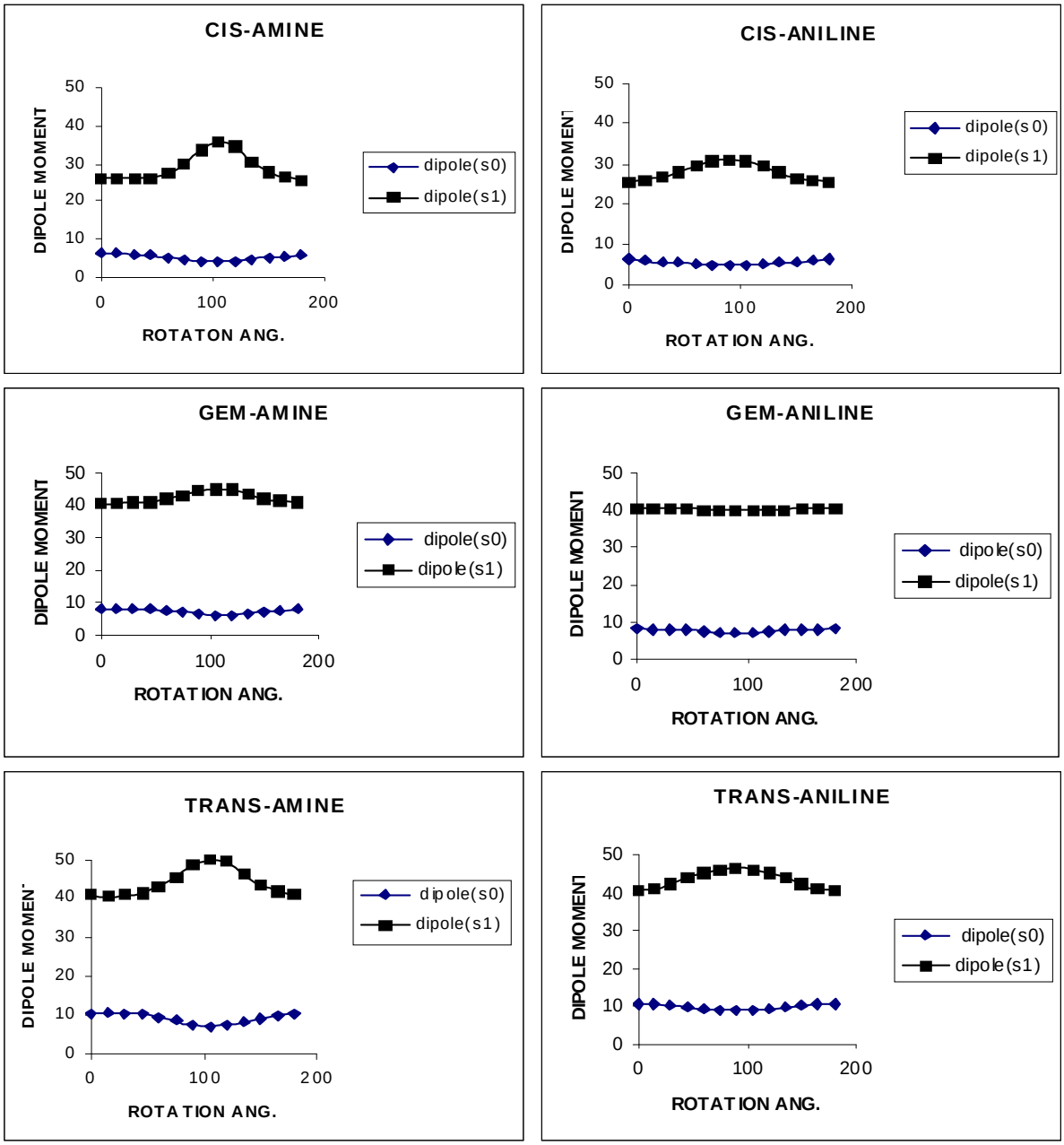

Figure 3.13. Ground and excited state dipole moments given as a function of rotation angle for all isomers of TEE derivative with NO_2

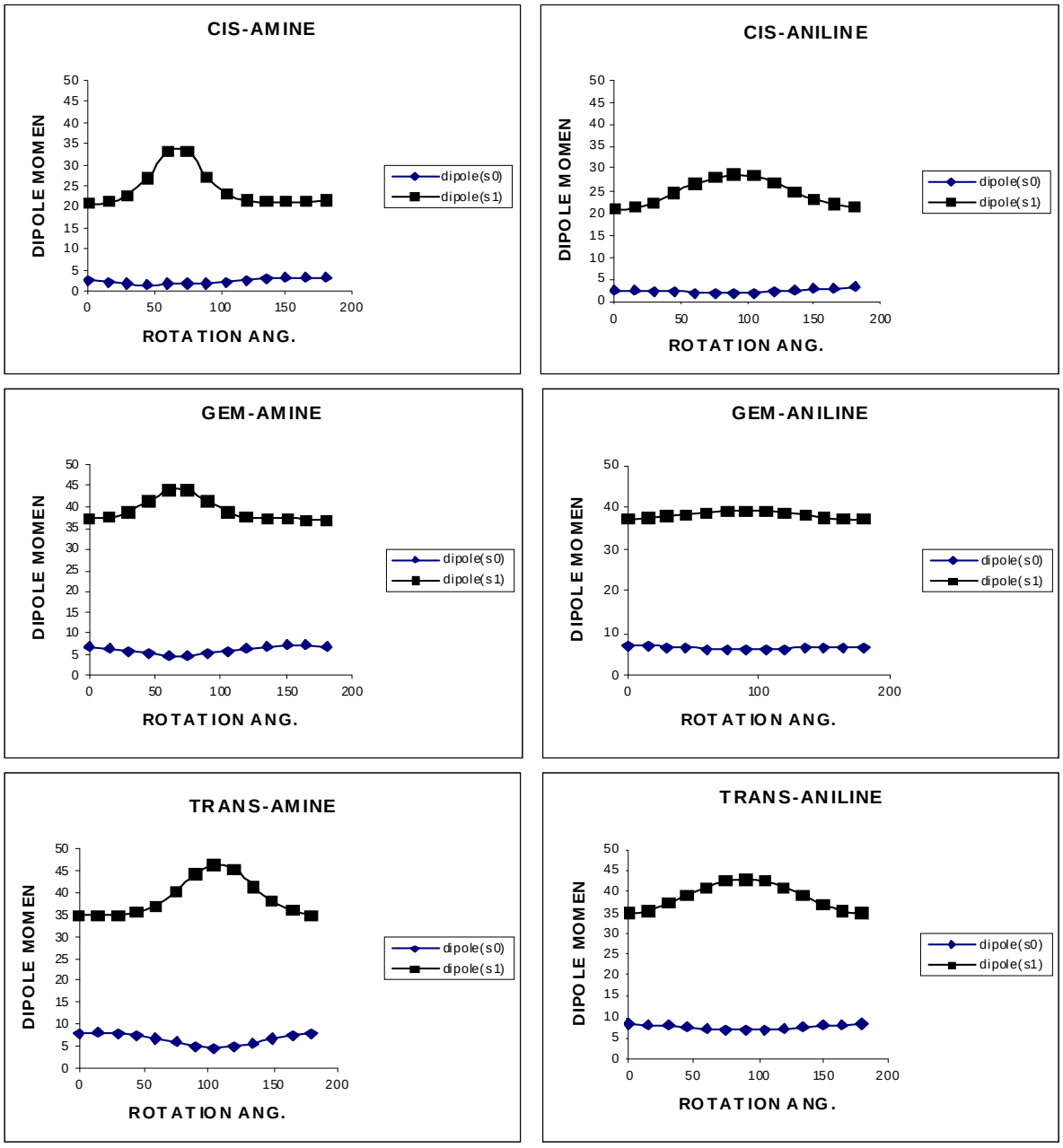

Figure 3.14. Ground and excited state dipole moments given as a function of rotation angle for all isomers of TEE derivative with CHO.

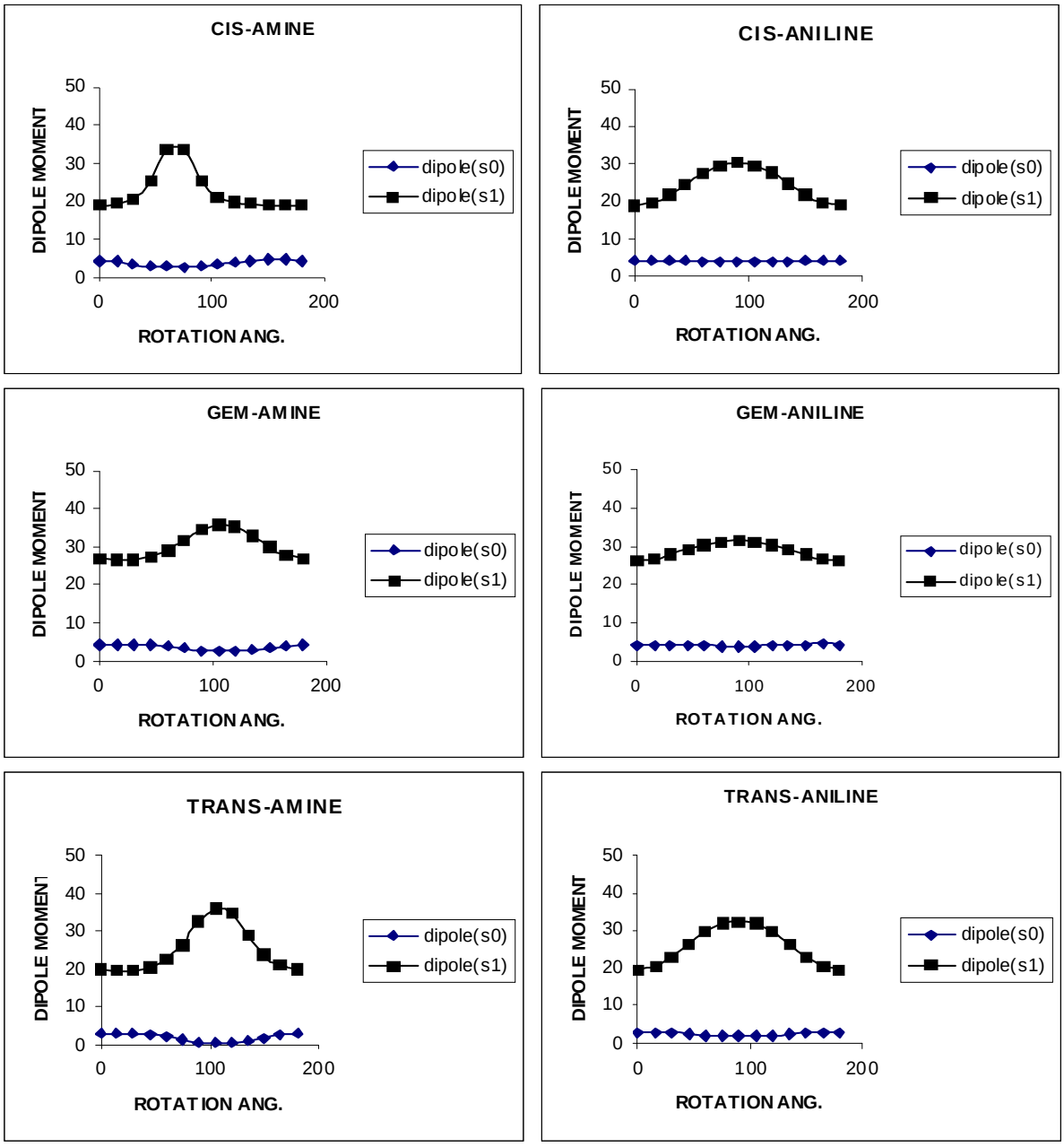

Figure 3.15. Ground and excited state dipole moments given as a function of rotation angle for all isomers of TEE derivative with CH_3

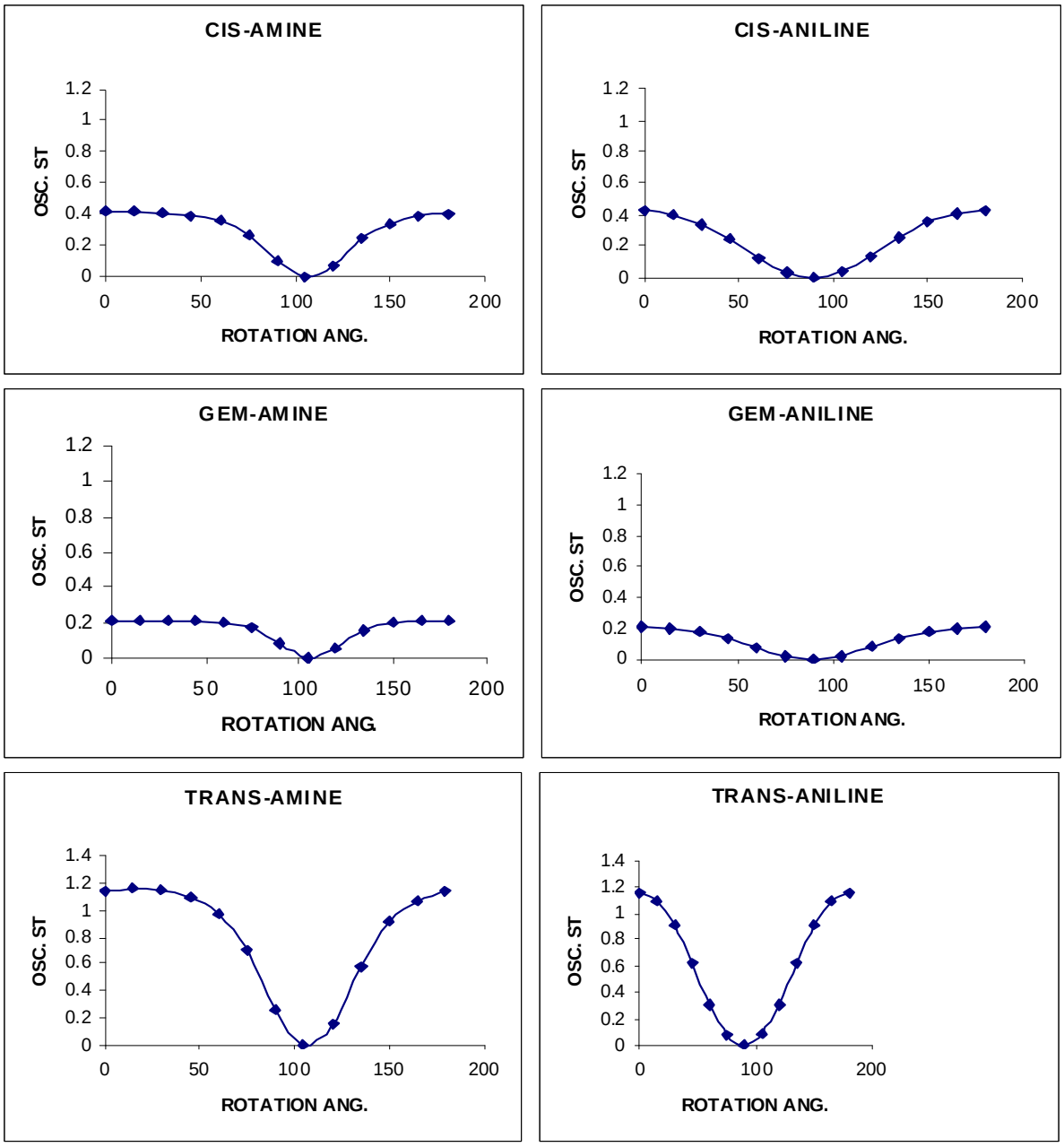

Figure 3.16. 1st Excited state oscillator strengths given as a function of rotation angle for all isomers of TEE derivative with NO_2

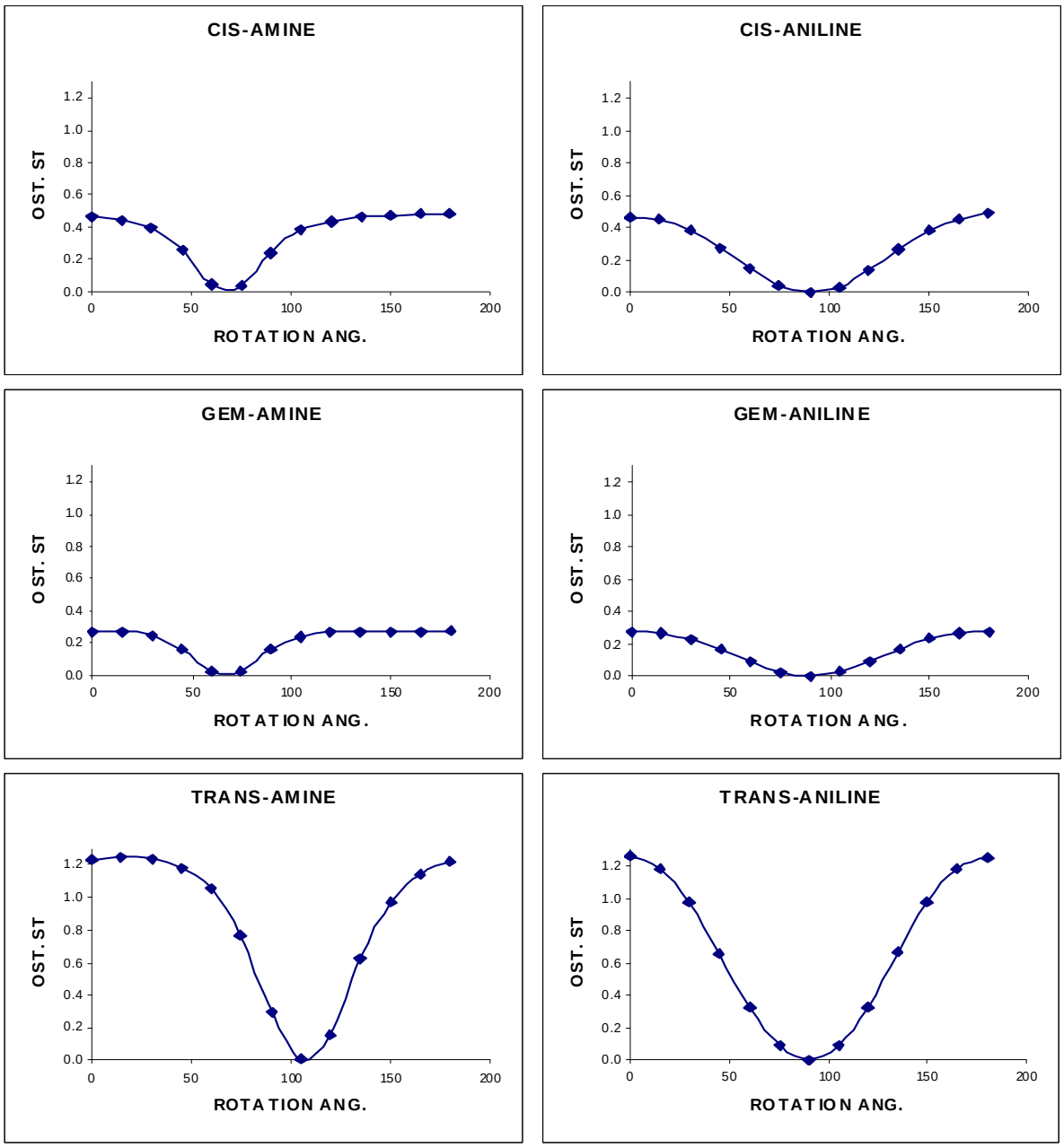

Figure 3.17. 1st excited state oscillator strengths given as a function of rotation angle for all isomers of TEE derivative with CHO

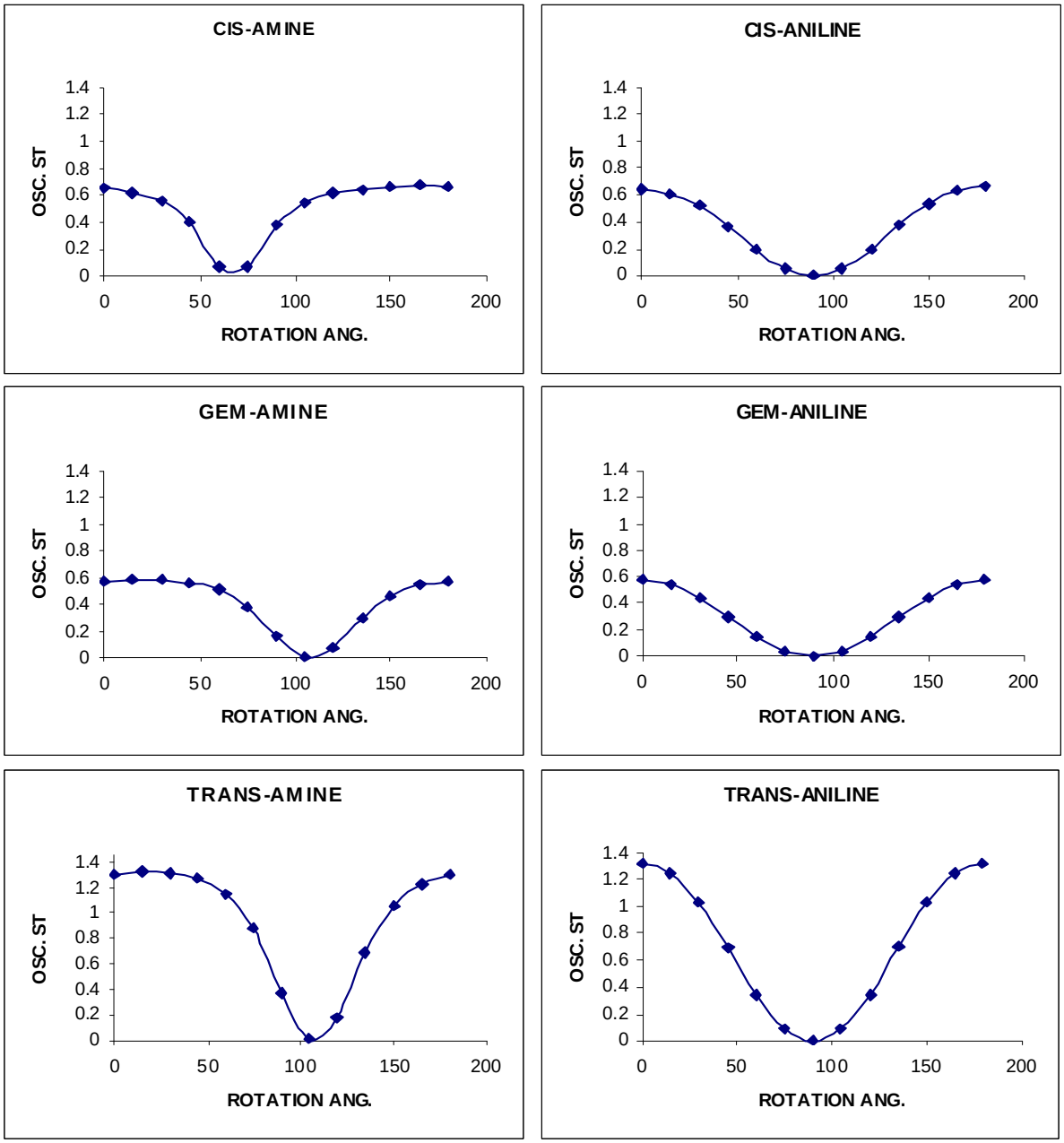

Figure 3.18 1st excited state oscillator strengths given as a function of rotation angle for all isomers of TEE derivative with CH_3

p-NO_2-benzene- substituted TEE derivatives:

Rotation of DMAmine group:

At 105º rotation angle, there is a maximum for the ground state energy and a minimum with a barrier for the first excited state for all isomers, cisT1, gemT2 and transT3* (see figure 3.10, 3.13, and 3.16). The barrier height is around 0.21-0.27 eV. The height of maximum at the ground state is nearly 0.45 eV. Oscillator strength reduces to zero at 105 degree. Oscillator strength is found higher than one (1) for trans isomer when the transition occurs to the 1st excited state from the most stable ground state structure as displayed in Figure 3.10.

The dipole moment at the 1st excited state varies between 40-45 D, while it changes about 7-8 D at ground state with respect to angle of rotation for gem isomers. It is hard to say there is a TICT state according these results, but this transition has a charge transfer character. The variation of dipole moment of Cis is 4-6 D at ground state, and about 26-36 at first excited state while the variation of dipole moment of Trans is 8-10 D at ground state, and 40-50 D at first excited state (See Figure 3.13). There is a maximum dipole value at first excited state, but a minimum dipole value at ground state for all isomers at 105º. The maximum dipole difference is observed between ground and first excited state for trans isomer for the twisted geometry. According to this result, we can say that trans isomer has a maximum charge transfer. This difference is minimum for cis, but nearly same for gem and trans isomers at locally excited state (this observation is also valid for rotation of DMA moiety).

Rotation of DMA group :

In the ground state graph, all isomers (Cis, Gem, Trans) have maximum value at a degree of 90-rotation angle, and they have without barrier minimum at the first excited state for this angle (Figure 3.10). Twisted configuration has 0.12-0.21 eV less energy than ground state configuration at the 1st excited state. The hill height at the ground state is not considerable it is only about 0.1 eV. Oscillator strength becomes zero at 90 degree (Figure 3.16).

There is no effect of rotation on the dipoles for both ground and 1st excited states of gem isomer. Dipole moment is about 40 D in the 1st excited state, 7-8 D in ground stat of gem isomer (Figure 3.13). These indicate that there is no TICT state while observing charge transfer for gem location. An increase of 20-25 D appears from ground state to the 1st excited state for cis whereas it is 30-35 D for trans isomers. The twisted structure possesses highest dipole at the excited state but lowest dipole at the ground state in 90 degrees.

p-CHO-benzene- substituted TEE derivatives:

Rotation of DMAmine group :

A local minimum followed by a shallow maximum is identified at 135 degree and 105 degree for cis-gem and trans isomers respectively at the 1st excited state energies. The barrier heights change between 0.20-0.23 eV. Although cis and Gem have local minimum, Trans has a maximum with nearly 0.43 eV heights for the above twist angles at ground state (Figure 3.11). There is big difference between ground and 1st excited state dipoles for all isomers with 30-40 D higher in excited state. We observe a maximum at 1st excited and minimum at ground state at 60-75 and at 105^{o} for Cis-gem and trans isomers respectively (Figure 3.14). At these angles oscillator strength diminishes. Even though there is no maximum excited state dipole at the angles where 1st excited state has a minimum energy, there is a wide plateau at the angles in which excited state dipole is highest for gem-cis cases. We accept the twist angle as 60-75 ^{o} for those by assuming that they prefer plateau. We met the same situation again, while we observe charge transfer TICT effect is blurry.

Rotation of DMA group:

All isomers have a very small maximum at 90 ^{o} for the ground state, and they have barrierless minimum for first excited state at this angle (Figure 3.11). Oscillator strength comes down to zero at 90 ^{o} (Figure 3.17) There is no change of dipole moment with the rotation angle for Gem at the ground and 1st excited states. Although dipoles in

excited state raise significantly compared to the ground state (charge transfer), there is no TICT effect for gem.

Once again dipole of 1st excited state is much higher than ground state for cis and trans. As shown in Figure 3.14 the highest charge transfer is in trans isomer.

p-CH_3-benzene- substituted TEE derivatives:

Rotation of DMAmine group:

In this type of compound, local minimums with a barrier appear at 135 ^{o} and 105^o rotation angle for cis and gem-trans the 1st excited state energies respectively (Fig.3.12.). Barrier height changes between 0.19-0.23 eV. Although in these twist angles Cis has a minimum, Trans and Gem have maximum with 0.41 eV higher at ground state. A plateau is observed at the 1st excited state energy however a maximum is seen at ground state energy when cis isomers twisted as 60-75 ^{o}. Variation of dipole moment with respect to angle changes between 27-36 D at excited state for Gem; it is about 3-4 D at ground state. While observing charge transfer, TICT effect is less than the other isomers. The dipole moment is 0-5 D for Cis and trans at ground state it is in between 19-36 D at excited state.

The dipole moment has greatest value in 60-75 ^{o}, 105 ^{o} for cis and Trans- Gem respectively at the 1st excited state. The opposite situation (lowest dipole) is observed for ground state. Oscillator strength vanishes to zero at these rotation angles.

Rotation of DMA group:

A maximum for ground and a minimum for 1st excited state at 90 ^{o} met in all isomers. Trans and Cis have minimum with a small barrier for first excited state at this angle (Figure 3.12.). TICT has 0.22 eV less energy than LE for gem. Oscillator strength reduces to zero at 90 degree (Figure 3.18) It has not been observed any change of dipole moment with the rotation angle at Gem. Dipole moment is about 26-31D in excited state, 4 D in ground state at Gem. The greatest dipole moment difference between ground state and first excited state is observed again for trans isomer at TICT state.

3.2.2 TEE Dimer

3.2.2.1 Ground State Behaviour

The information about the ground state energy and geometry of mono DMA substituted TEE dimers are given table 3.23 and figure 3.19 figure. Two TEE units are the same plane in trans conformer but one TEE unit is 53 degrees rotated w.r.t the other in cis conformer. The ground states energies of two conformers are extremely close each other though cis has lower energy. (See table 3.23)

Table 3.23 The ground state energies and the structural parameters of mono DMA substituted TEE dimers

Substance	**Between two**	**Between amine**	**Energy/au**	**sp^2-sp^2**	**sp^2-sp**
	centers dihedral ang.	**anilino dihedral ang.**		**Double/** Å	**Single/** Å
1trans	180	-53	0.7859738	1.374	1.40
1cis	148	-53	0.7858525	1.374	1.40

Structure	HOMO	LUMO
1cis 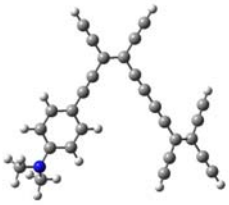	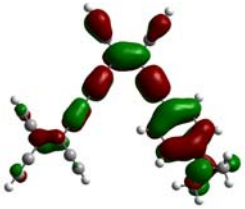	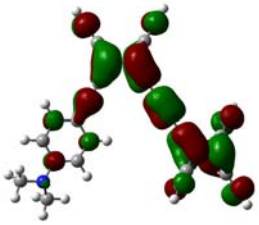
1trans 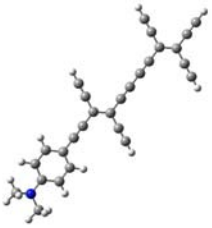	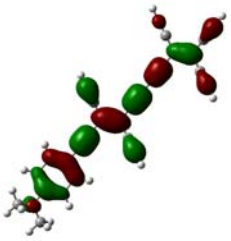	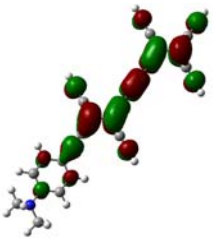

Figure 3.19 HOMO-LUMO structures of mono DMA substituted TEE dimers

3.2.2.2 Excited State Behavior

We performed excited state calculations on AM1 ground state geometry of DMA substituted TEE dimer. The excited state calculations for twisted DMA unit by 90 degrees out of the TEE plane is used to understand TICT behaviour for cis and trans isomers.

When we look into HOMO-LUMO structures DMA moiety acts like an electron donor and TEE unit located at the other end of the molecule behave like an electron acceptor in cis conformer. However the electron migration takes place from the benzene ring of anilino unit toward to the two TEEs of dimer in trans.

The transition to the 1st excited state appears at 516 nm with 1.3 oscillator strength and primarily H to L nature for the local excitation for trans isomer. On the

other hand twisted one, gives 560 nm λ_{max} with zero oscillator strength, H;L dominant nature and 10 D higher in dipole moment.

We observe the similar situation for cis isomer where λ_{max} is 539 nm (F=0.4) and 566 nm(F=0) ground and twisted structures. The dipole increase is 6D.

The red shift is 44 nm in trans while 27 nm in cis compound. All the above observations are a sign of the existence of TICT state in both isomers but we expect more solvent effect on the trans isomer.

Table 3.24 First excited state properties with rotation angle for trans isomer of mono DMA substituted TEE dimers

ROT.ANG	ExE(s1)eV	λ_{max}	osc.st	dipole(s0)	dipole(s1)
0	2.4004	516.51	1.3007	5.0537	35.6234
90	2.2145	559.86	0	3.6485	46.6745

Table 3.25 First excited state properties with rotation angle for cis isomer of mono DMA substituted TEE dimers

ROT.ANG	ExE(s1)eV	λ_{max}	osc.st	dipole(s0)	dipole(s1)
0	2.2992	539.26	0.4277	4.217	26.5891
90	2.1906	565.97	0	3.2384	33.1404

We expect that when more than one unit of DMA is attached on TEE dimer, λ_{max} would increase though the experimental end absorption is around 660nm tetra of DMA substituted TEE dimer [35].

CONCLUSION

The above results can be summarized as follows: All radialenes and expanded radialenes have a planar structure except the size of six which has usually a three dimensional chair like structure. There is no correlation found between bond lengths and the size of radialenes and expanded ones. All of the methods used give the same results.

The transition from the ground state to the first excited state is predominantly H-L transition, and although ground state dipole moment is zero for all of them, excited state dipoles differ from zero for odd sized radialenes and expanded radialenes. If the transition to the 1st excited state is forbidden and different than that of H to L, the next allowed transition is primarily H-L transition.

Expanded radialenes with general formula of $C_{10}H_{2n}$ have maximum absorption around 540-600 nm, the similar kind of a derivative which is tetra $N(C_{12}H_{25})_2$anilino substituted gives 750 nm max wavelength experimentally.

Expanded radialenes with size 2 have largest wavelength; its transition nature is not the expected H to L, but rather H-1 to L. There is no electron density on the bonds outside of the ring in the H-1 orbitals, hence the transition involved from triple bonds inside the ring to the outside.

Most of the frontier MO's orbitals are doubly degenerate, the allowed transitions and some of 1st excited state transitions contain doublets that may be the source of the huge molar absorbtivities (ε) which is the related to the intensities of electronic absorption peaks.

According to results of TEE monomer derivatives, oscillator strength is determined higher than one for all of trans isomers when the transition occurs to the 1st excited state from the most stable ground state structure. On the other hand all trans isomer have the maximum dipole difference between ground and first excited state for the twisted geometry.

In all isomers of push-pull TEE monomers that we investigated; λ_{max} value decreases from NO_2 substitued to CH_3 substituted; in other word λ_{max} value increases with increasing acceptor strength. The TICT state is found clearly in all cis and trans

isomers when anilino moiety is twisted. However for amine rotation, it is blurry that there exists such a state.

Bond lengths do not change for acyclic and cyclic TEE derivatives.

All the observations related to mono -DMA substituted TEE dimers are a sign of the existence of TICT state in trans and cis isomers. Trans isomer has oscillator strength higher than one. There is a linear conjugation in trans isomer while the others also have cross conjugation, which delocalizes conjugation path in two dimensions. The dipole difference from the ground state structure is much more for trans, so that we expect the solvent effect will be more in that isomer. All of our results are in consistent with the recorded experimental ones.

REFERENCES

[1] F. Diederich, “Carbon Scaffolding Acetylenic All-Carbon and Carbon-Rich Compounds”, *Nature (London),* **369**, (1994), 199-207.

[2] M. Schreiber, R. R. Tykwinski, F. Diederich, R. Spreiter, U. Gubler, C. Bosshard, I. Poberaj, P. Günter, C. Boudon, J.-P. Gisselbrecht, M. Gross, U. Jonas, H. Ringsdorf, "Tetraethynylethene Molecular Scaffolding: Nonlinear Optical, Redox, and Amphiphilic Properties of Donor Functionalized Polytriacetylene and Expanded Radialenes ", *Adv. Mater.,* **9**, (1997), 339-343.

[3] M. Schreiber, J. Anthony, F. Diederich, M. E. Spahr, R. Nesper, M. Hubrich, F. Bommeli, L. Degiorgi, P. Wachter, P. Kaatz, C. Bosshard, P. Günter, M. Colussi, U. W. Suter, C. Boudon, J.-P. Gisselbrecht, M. Gross. “Polytriacetylenes: Conjugated Polymers with a Novel all-carbon backbone”, *Adv. Mater*., **6**, (1994), 786.

[4] F. Diederich, Y. Rubin, “Synthetic Approaches toward Molecular and Polymeric Carbon Allotropes”, *Angew. Chem*., **104**, (1992), 1123-1146; *Angew. Chem. Int. Ed. Eng.,* **31,** (1992), 1101-1123.

[5] Y. Hori, K. Noda, S. Kobayashi, H. Taniguchi, “Synthesis and Properties of Tetrakis (phenylethynyl) ethylene”, *Tetrahedron Lett*., (1969), 3563-3566.

[6] H. Hauptmann, “Tetraethynylethylenes ”, *Angew. Chem*., **87** (1975), 490-491; *Angew. Chem. Int. Ed. Engl*., **14**, (1975), 498-499.

[7] H. Hauptmann, “Untersuchungen zu Baseninduzierten Reaktionen and etraäthinyläthanen”, *Tetrahedron Lett*., (1975), 1931-1934.

[8] H. Hauptmann, “Diäthinylcarbene und 2,4-Pentadiinylidene”, *Tetrahedron,* **32,** (1976), 1293-1297.

[9] Y. Rubin, C. B. Knobler, F. Diederich, “Tetraethynylethylene”, *Angew. Chem.,* **103**, (1991), 708-710 ; *Angew. Chem. Int. Ed. Engl.,* **30**, (1991), 698-700.

[10] R. R. Tykwinski, F. Diederich, “Tetraethynylethylene Molecular Scaffolding”, *Liebigs Ann./Recuel.,* (1997), 649-661.

[11] F. Diederich, in Modern Acetylene Chemistry; P.J. Stang, F. Diederich,(Eds.), Verlag Chemie: Weinheim, 1995; Chapter 13. Oligoacetylenes.

[12] F. Diederich, L. Gobbi, ”Cyclic and Linear Acetylenic Molecular Scaffolding”, *Top. Curr. Chem*., **201**, (1998), 44-79.

[13] J. D. Van Loon, P. Seiler, F. Diederich, “Tetrakis(trialkylsilylethynyl) butatriene and 1,1,4,4,-Tetrakis(trialkylsilylethynyl)-1,3-butadine: Novel Cross-Conjugated Chromophores”, *Angew. Chem*., **105**, (1993), 1235-1238; *Angew. Chem. Int. Ed. Engl*., **32**, (1993), 1187-1189.

[14] J. Anthony, C. B. Knobler, F. Diederich, “Stable [12] and [18] Annulenes Derived from Tetraethynylethylene”, *Angew. Chem.,* **105**, (1993), 437-440; F. Diederich, *Angew. Chem. Int. Ed. Engl.*, **32**, (1993), 406-409.

[15] A. M. Boldi, F. Diederich, ”Expanded Radialenes: A Novel Class of Cross-Conjugated Macrocycles”, *Angew. Chem.,* **106**, (1994), 482-485; Angew. *Chem. Int. Ed. Engl.,* **33**, (1994), 468-471.

[16] J.Anthony, A.M. Boldi, C. Boudon, J.P. Gisselbrecht, M. Gross, P. Seiler, C.B. Knobler, F. Diederich, ”Macrocylic Tetraethynylethene Molecular Scaffolding: Perethynylated Aromatic Dodecadehydro[18]annulenes, Antiarmatic Octadehydro[12]annulenes, and Expanded Radialenes”, *Helv.Chim. Acta.,* **78**, (1995), 797-817.

[17] T. Lange, V. Gramlich, W. Amrein, F. Diederich, M. Gross, C. Boudon, J.P. Gisselbrecht,”Hexakis(trimetylysilyl)[3]radialene: A Carbon-Rich Chromophone with Unusual Electronic Properties”, *Angew. Chem.,* **107,** (1995)**,** 898-901; *Angew. Chem. Int. Ed. Engl.,* **34**, (1995), 805-809.

[18] A. M. Boldi, J. Anthony, C. B. Knobler, F. Diederich, ”Novel Cross-Conjugated Compounds Derived from Tetraethynylethene”, *Angew. Chem.,* **104**, (1992)**,** 1270-1273; *Angew. Chem. Int. Ed. Engl.,* **31**, (1992), 1240-1242.

[19] J.Anthony, A.M. Boldi, Y. Rubin, M. Hobi, V. Gramlich, C.B. Knobler, P. Seiler, F. Diederich, “Tetraethynylethenes: Fully Cross-Conjugated π-Electron Chromophones and Molecular Scaffolds for All-Carbon Networks and Carbon-Rich Nanomaterials”, *Helv.Chim. Acta.,***78**, **(**1995), 13-45.

[20] A.M. Boldi, J.Anthony, V. Gramlich, C.B. Knobler, C. Boudon, J.P. Gisselbrecht, M. Gross, F. Diederich, “Acyclic Tetraethynylethene Molecular Scaffolding: Multinanometer-Sized Linearly Conjugated Rods with the Poly(triacetylene) Backbone and Cross-Conjugated Expanded Dendralenes”, *Helv.Chim. Acta*., **78**, (1995) 779-796.

[21] J.Anthony, C. Boudon, F. Diederich, J.P. Gisselbrecht, V. Gramlich, M. Gross, M. Hobi, P. Seiler, *Angev.Chem.* “Stable Soluble Conjugated Carbon Rods with a Persilylethynylated Polytriacetylene Backbone”, *Angew. Chem.,* **106**, (1994), 794-798; *Angew. Chem. Int. Ed. Engl.,* **33**, (1994), 763-766.

[22] J. Anthony, “Cross Conjugated Carbon-Rich Compounds”, *Ph.D. Thesis*, University of California, Los Angeles, (1993).

[23] R.E. Martin, U. Gubler, C. Boudon, V. Gramlich, C. Bosshard, J.P. Gisselbrecht, P. Günter, M. Gross, F. Diederich, "Poly(triacetylene) Oligomers: Synthesis, Characterization, and Estimation of the Effective Conjugation Length by Electrochemical, UV/Vis, and Nonlinear Optical Methods", *Chem. Eur. J.,* **3**, (1997), 1505-1512.

[24] D. H. Waldeck, "Photoisomerization Dynamics of Stilbenes", *Chem. Rev.,* 91, (1991), 415-436.

[25] M.O. Wolf, H. H. Fox, M. A. Fox, "Reduction of Acetylated Tetraphenylethylenes: Electrochemical Behavior and Stability of the Related Reduced Anions", *J. Org. Chem*., **61, (**1996), 287-294.

[26] R. R. Tykwinski, M. Schreiber, R. Perez Carlon, F. Diederich, V. Gramlich, "Donor/Acceptor-Substituted Tetraethynylenes: Systematic Assembly of Molecules for Use as Advanced Materials", *Helv. Chim. Acta.,* **79**, (1996), 2249-2281.

[27] R. R. Tykwinski, M. Schreiber, V. Gramlich, P. Seiler, F. Diederich, "Donor-Acceptor Substituted Tetraethynylethenes", *Adv. Mater*., **8**, (1996), 226-231.

[28] H. Hopf, M. Kreutzer, P. G. Jones, "Zur Darstellung und Structur von Tetrakis(phenylathinyl)ethene", *Chem. Ber*., **124**, (1991), 1471-1475.

[29] C. Boudon, J.P. Gisselbrecht, M. Gross, J. Anthony, A.M. Boldi, R. Faust, T. Lange, D. Philp, J.D. Van Loon, F. Diederich, "Electrochemical Properties of Tetraethynylethenes, Fully Cross-Conjugated π-Chromophores, and Tetraethynylethene-Based Carbon-Rich Molecular Rods and Dehydroannulenes", *J. Electroanal. Chem.,* **394**, (1995), 187-197.

[30] A. Hilger, J. P. Gisselbrecht, R. R. Tykwinski, C. Boudon, M. Schreiber, R. E. Martin, H. P. Luethi, M. Gross, F. Diederich, "Electronic Characteristics of Arylated Tetraethynylethenes: A Cooperative Computational and Electrochemical Investigation", *J. Am. Chem. Soc.,* **119**, (1997), 2069-2078.

[31] C. Bosshard, R. Spreiter, P. Günter, R. R. Tykwinski, M. Schreiber, F. Diederich, "Structure-Property Relationship in Nonlinear Optical Tetraethynylethenes", *Adv. Matter.,* **8**, (1996), 231-234.

[32] R. Spreiter, C. Bosshard, G. Knöpfle, P. Günter, R. R. Tykwinski, M. Schreiber, F. Diederich, "One- and two- Dimentionally Conjugated Tetraethynylethenes: Structure versus Second-Order Optical Polarizabilities *", J. Phys. Chem. B.,* **102**, (1998), 29-32.

[33] U. Gubler, R. Spreiter, C. Bosshard, P. Günter, R. R. Tykwinski, F. Diederich, "Two-Dimensionally Conjugated Molecules: The Importance of Low Molecular Symmetry for Large Third-Order Nonlinear Optical Effects", *Appl. Phys. Lett.,* **73**, (1998), 2396-2398.

[34] R. R. Tykwinski, U. Gubler, R. E. Martin, F. Diederich, C. Bosshard, P. Günter, J. "Structure-Property Relationship in Third-Order Nonlinear Optical Chromophores", *Phys. Chem. B*., 1**02**, (1998), 4451-4465.

[35] M. B. Nielsen, M. Schreiber, Y. G. Baek, P. Seiler, S. Lecomte, C. Boudon, R. R. Tykwinski, J. P. Gisselbrecht, V. Gramlich, P. J. Skinner, C. Bosshard, P. Günter, M. Gross, and F. Diederich, "Highly Functionalized Dimeric Tetraethynylethenes and Expanded Radialenes: Strong Evidence for Macrocyclic Cross-Conjugation", *Chem. Eur. J.,* **7**, (2001), 3263.

[36] F. Diederich, "Design and Synthesis of Functional Molecular Architecture", *Chimia,* **55**, (2001), 821-827.

[37] G. Köbrich, H. Heinemann, "Tri(isopropylidene)cyclopropane", *Angew. Chem. Int. Ed. Engl.,* **4**, (1965), 594-595.

[38] Ernest A. Dorko, "The Preparation and Properties of Trimethylenecyclopropane", *J. Am. Chem. Soc*., **87**, (1965), 5518 – 5520.

[39] Gary W. Griffin and Laurence I. Peterson, "The Chemistry of Photodimers of Maleic and Fumaric Acid Derivatives. IV. Tetramethylenecyclobutane", *J. Am. Chem. Soc.,* **85**, (1962), 3398 – 3400.

[40] A. J. Barkovich, E. S. Strauss, and K. P. C. Vollhardt, "Hexaradialene", *J. Am. Chem. Soc.,* **99**, (1977), 8321 – 8322.

[41] Lewis G. Harruff, Mark Brown, and Virgil Boekelheide, "Hexaradialene: precursors and structure", *J. Am. Chem. Soc.,* **100**, (1978), 2893 – 2894.

[42] H. Hopf, G. Maas, "Preparetion and Properties, reactions, and Applications of Radialenes", *Angew. Chem.,* **104, (**1992), 953-977; *Angew. Chem. Int. Ed. Engl.,* **31**, (1992), 931-954.

[43] Maas, G.; Hopf, H. "In The chemistry of the dienes and polyenes", *Angew. Chem. Int. Ed. Engl., **31,*** (1992), 931-954.

[44] Michael J. S. Dewar and Gerald Jay Gleicher, "Ground States of Conjugated Molecules. III. Classical Polyenes", *J. Am. Chem. Soc.,* **87**, (1965), 692 – 696.

[45] T. Sugimoto, Y. Misaki, T. Kajita, Z. Yoshida, Y. Kai, N. Kasai, "Hexakis (1,3-dithio-2-ylidene)cyclohexane with two different conformations of the six-membered ring", *J. Am. Chem. Soc.,* **109**, (1987), 4106-4107.

[46] F. Diederich, "Functional acetylenic molecular architecture", *Pure & Appl. Chem.***, 71**, (1999), 265–273.

[47] Nielsen MB, Diederich F, "The art of acetylenic scaffolding: Rings, rods, and switches", *Chem. Rec.,* **2**, (2002), 189-198.

[48] **D**. W. Rogers and F. J. McLafferty, "G3(MP2) Calculations of Enthalpies of Hydrogenation, Isomerization, and Formation of [3]-Radialene and Related Compounds", *J. Phys. Chem. A.,* **106***,* (2002)**,** 1054-1059.

[49] F. Diederich (1997) "Tetraethynylethenes:Versatile Carbon-Rich Building Blocks for Two-Dimensional Acetylenic Scaffolding", *J. Michel*, Modular Chemistry, Kluver, Dordrecht, (1997), 17.

[50] F. Diederich, D. Philp, P. Seiler, "π-Complexes Incorporating Tetraphenyltetraethynylethene", *J. Chem. Soc., Chem. Commun*., (1994), 205-208.

[51] D. Philp, V. Gramlich, P. Siler, F. Diederich, "π-Complexes :Incorporating Tetrakis(phenylethynyl)ethane", *J. Chem. Soc.,* (1995), 875-886.

[52] H. Taniguchi, K. Hayashi, K. Nishioka, Y. Hori, M. Shiro, T. Kitamura, "A new Type of Inclusion Compounds Composed of a Charge-Transfer Complex between Tetrakis(phenylethynyl)ethene and 2,4,6-Trinitrofluorenone", *Chem. Lett*., **1994**, 1921-1924.

[53] B. Ma, Y. Xie, H. F. Schaefer III, "Tetraethynylethylene, A Molecule with Four Very Short C-C Single Bonds. Interpretation of the Infrared Spectrum", *Chem. Phys. Lett*., **6**, (1992), 521-526.

[54] B. Ma, H. M. Sulzbach,Y. Xie, H. F. Schaefer III, "π-Electron Delocalization and Compression in Acyclic Acetylenic Precursors to Multidimensional Carbon Networks: Comparison with Experiment for the Recently Synthesized Tris(trimethylsilyl)-Substituted Tetraethynylmethane.

Structures, Thermochemistry, Infrared Spectra, Polarizabilities, and Hyperpolarizabilities", *J. Am. Chem. Soc*., **116**, (1994), 3529-3538.

[55] T. Höpfner, P. G. Jones, B. Ahrens, I. Dix, L. Ernst, and H. Hopf, "[6]Radialenes Revisited", *Eur. J. Org. Chem.,* **9**, (2003), 2596-2611.

[56] D. J. Eluvathingal , K. P. Ashwini, R. Uwe, "Structure and bonding of metallacyclocumulenes, radialenes, butadiyne complexes and their possible interconversion: a theoretical study", *Journal of Organometallic Chemistry,* **635,** (2001), 204–211.

[57] M Iyoda, Nobuko Nakamura,a Mie Todaka, Shinya Ohtsu, Kenji Hara, Yoshiyuki Kuwatani, Masato Yoshida, Haruo Matsuyama, Masaki Sugita, Hiroshi Tachibana and Haruo Inoue, "Novel synthesis of hexaaryl[3]radialenes via dibromo[3]dendralenesy", *Tetrahedron Letters*, **41**, (2000), 7059-7064.

[58] K. Matsumoto, Y. Harada, T. Kawase and M. Oda, "Hexakis(2-pyridyl)- and hexakis(3-pyridyl)[3]radialene: novel, water-soluble [3]radialenes with potential utility for supramolecular chemistry", *Chem. Commun.,* (2002), 324–325.

[59] M. Traetteberga, P. Bakkena, H. Hopf, Thomas Höpfner, "The molecular structure of a [6]radialene: a gas electron diffraction and ab initio study of hexakis(ethylidene)-cyclohexane", *Journal of Molecular Structure,* **44**, (1998) 99-105.

[60] *http://www.darpa.mil/mto/mole/molecomp.htm*

[61] R. J. Mitchell, "*Microprocessor Systems: An Introduction" Macmillan*, London, (1995).

[62] *http:// www.physics.purdue.edu/nanophys/molecule.htm*

[63] K. Müllen, G. Wegner, “Electronic Materials: the Oligomer Approach”, *Wiley-VCH,* Weinheim, (1997).

[64] B. L Feringa, “Molecular Switches” *Wiley/VCH*, Weinheim, Germany, (2001).

[65] M. Irie, "Photochromism: memories and switches", *Chem. Rev.*, **100,** (2000), 1683-1890.

[66] L. Gobbi, P. Seiler, F. Diederich, V. Gramlich, “Molecular Switching: A Fully Reversible, Optically Active Photochemical Switch Based on a Tetraethynylethene-1,1-Binaphthalene Hybrid System”, *Helv. Chim. Acta*., **83**, (2000), 1711-1723.

[67] F. M. Raymo and S. Giordani, “All-optical processing with molecular switches”, *Jack Halpern*, University of Chicago, Chicago, IL, 2002.

[68] E. Lippert, W. Lüder, H. Boos, “In Advances in Molecular Spectroscopy, Proceedings of the 4th International Meeting on Molecular Spectroscopy”, *A. Mangini*, Pergamon, Oxford, (1962), 443 -457.

[69] Z. R. Grabowski, K. Rotkiewicz and W. Rettig, “Structural Changes Accompanying Intramolecular Electron Transfer: Focus on Twisted Intramolecular Charge-Transfer States and Structures”, *Chem. Rev.,* **103**, (2003)**,** 3899-4031.

[70] Z. R. Grabowski, K. Rotkiewicz, A. Siemiarczuk, D. J. Cowley, and W. Baumann, “Twisted intramolecular charge transfer states (TICT).A new class of excited states with a full charge separation”, *Nouv. J. Chim., (New J. Chem)* **3**, (1979). 443.

[71] Z. R. Grabowski and J. Dobkowski, "Twisted intramolecular charge transfer states (TICT) excited states: Energy and molecular structure", *Pure Appl. Chem*., **55**, (1983), 245.

[72] W. Rettig and W. Baumann, "Luminescent and nonluminescent twisted intramolecular charge transfer states (TICT) excited states: Dipole moment and application, in: Photochemistry and Photophysics", *J. F. Rabek*, Boca Raton, Florida **6**, (1992), 79-134.

[73] Z.R. Grabowski, K. Rotkiewicz, and W. Rettig, "Structural changes accompanying intramolecular electron transfer–focus on T.I.C.T. states and structures", *Chem. Rev.,* **103,** (2003), 3899-4031.

[74] W. Retting, "Anwendungsaspekte adiabatischer Photoreaktionen", *Nachr. Chem. Tech. Lab*., **39,** (1991), 298.

[75] K. A. Al-Hassan and W. Retting, "Free volume sensing fluorecent probes", *Chem. Phys. Lett*., **126,** (1986), 273.

[76] W. Retting, R. Fritz, and J. Springer, "Fluorescence probes based on adiabatic photochemical reactions, in: Photochemical Process in Organized Molecular Systems" , Elsevier Science Publishers, Amsterdam, (1991), 61.

[77] W. Retting, "Kinetic studies on fluorescence probes using synchrotron radiation, in: Fluorescence Spectroscopy: New Methods and Applications", *O. S. Wolfbeis*, Springer-Verlag, Berlin, (1993), 31-47.

[78] L. Gobbi, N. Elmaci, H. P. Luthi, F. Diederich, "N,N-Dialkylaniline-Substituted tetraethynylethenes: A new class of chromophores possessing an emitting charge-transfer state. Experimental and computational studies ", *chemphyschem.,* **2**, (2001), 423- 433.

[79] David Young, “Computational Chemistry: A Practical Guide for Applying Techniques to Real-World Problems”, *A John Wiley & Sons*, Inc, New York, 2001.

[80] Frank Jensen, “Introduction to Computational Chemistry”, *A John Wiley & Sons,* Chishester, 1999.

[81] A. Szabo, N. S. Ostlund, “Modern Quantum Chemistry: Introduction Advanced Electronic Structure Theory”, *Macmillan Publishing*, New York, 1982.

[82] M. J. S. Dewar, E. G. Zoebisch, E. F. Healy, J. J. P. Stewart, “AM1: A New General Purpose Quantum Mechanical Molecular Model”, *J. Am. Chem. Soc.,* **107**, (1985), 3902-3909.

[83] J. Ridley, M. C. Zerner, “An Intermediate Neglect of Differential Overlap Technique for Spectroscopy: Pyrrole and the Azines”, *Theor. Chim. Acta*., **32**, (1973), 111-134.

[84] A. Nagy, “Density functional Theory and application to atoms and molecules”, *Physics Reports.,* **298,** (1998), 1-79.

[85] A. D. Becke*,* ”A New Mixingof Hartree-Fock and Local Density-Functional Theories”*, J. Chem. Phys.,* **98**, (1993), 1372-1377.

[86] Neepa T. Maitra and Kieron Burke, “Memory in Time-Dependent Density Functional Theory”, *Physical Review Letter,* **89**, (2002), 23002.

[87] C. D. Ritche, “Phisical Organic Chemistry: The Fundamental Concepts”, *Dekker,* New Yourk, (1990).

APPENDIX A

Table A.1. The first excited state properties of radialenes and expanded radialenes for TDDFT/3-21G//DFT /6-31G* calculations.

Substance	ExE(s1)eV	lmax	osc.st	dipole(s0)	dipole(s1)
3a	5.011	247	0.326	0.00	4.19
4a	4.068	305	0.000	0.00	0.00
5a	3.671	338	0.000	0.00	7.23
6a	4.116	301	0.045	0.00	0.00
3b	4.141	299	0.090	0.00	9.08
4b	3.772	329	0.000	0.00	0.01
5b	3.655	339	0.000	0.00	14.92
6b	3.575	347	0.000	0.00	0.00
3c	2.659	466	0.262		
4c	2.397	517	0.000		
5c	2.327	533	0.000		
6c	2.131	582	0.035		
2d	2.783	445	0.000	0.00	0.00
3d	3.452	359	0.000	0.00	0.01
4d	3.354	370	0.000	0.00	0.00
5d	3.348	370	0.000	0.00	21.30
6d	3.312	374	0.000	0.00	0.05
2e	2.297	540	0.000	0.00	0.00
3e	2.395	518	0.457	0.01	13.25
4e	2.226	557	0.000	0.00	0.00
5e	2.175	570	0.000	0.00	24.16
6e	2.179	569	0.015	0.00	

Table A.2. The first excited state properties of radialenes and expanded radialenes for TDDFT/3-21G//DFT /3-21G* calculations.

Substance	ExE(s1)eV	lmax	osc.st	dipole(s0)	dipole(s1)
3a	5.092	243	0.324	0.00	4.23
4a	4.156	298	0.000	0.00	0.00
5a	3.719	333	0.000	0.00	7.23
6a	4.235	293	0.049	0.00	
3b	4.180	297	0.095	0.00	9.10
4b	3.793	327	0.000	0.00	0.02
5b	3.672	338	0.000	0.00	14.90
6b	3.586	346	0.000	0.00	0.00
2d	2.800	443	0.000	0.00	0.00
3d	3.200	388	0.000	0.00	0.00
4d	3.369	368	0.000	0.00	0.00
5d	3.351	370	0.000	0.00	21.27
6d	3.317	374	0.000	0.00	
2e	2.344	529	0.000	0.00	0.00
3e	2.401	516	0.454	0.00	13.20
4e	2.229	556	0.000	0.00	0.00
5e	2.177	570	0.000	0.00	24.06
6e	3.391	366	0.000	0.00	

Table A.3. The first excited state properties of radialenes and expanded radialenes for TDDFT/3-21G//DFT /AM1 calculations.

Substance	ExE(s1)eV	lmax	osc.st	dipole(s0)	dipole(s1)
3a	5.184	239	0.330	0.00	4.17
4a	4.153	299	0.000	0.00	0.00
5a	3.665	338	0.000	0.00	7.16
6a	3.908	317	0.038	0.00	0.03
3b	4.213	294	0.093	0.00	9.02
4b	3.809	326	0.000	0.00	0.00
5b	3.671	338	0.000	0.00	14.79
6b	3.573	347	0.000	0.00	0.08
2d	2.860	434	0.000	0.00	0.00
3d	3.257	381	0.000	0.01	0.02
4d	3.453	359	0.000	0.00	0.00
5d	3.414	363	0.000	0.00	21.20
6d	3.472	357	0.018	0.00	0.00
2e	2.272	546	0.000	0.00	0.00
3e	2.526	491	0.489	0.00	13.12
4e	2.356	526	0.000	0.00	0.01
5e	2.360	525	0.002	0.49	20.90
6e	3.472	357	0.018	0.00	0.00

Table A.4. Ground state energies of radialenes and expanded radialenes for different* calculations.

Substance	AM1/au	DFT-321G*/au	DFT-6-31G*/au
3a	0.1681097	-230.8284389	-232.1136379
4a	0.1665119	-307.848958	-309.5547539
5a	0.140982	-384.8628383	-386.9885034
6a	0.1676596	-461.83288	-464.381171
3b	0.4068088	-458.0651489	-460.6003675
4b	0.4635876	-610.8012378	-614.1809439
5b	0.5545697	-763.5185309	-767.7425325
6b	0.6627112	-916.2236833	-921.2913898
3c	0.9309489	-912.4219191	-917.4698301
4c	1.1616748	-1216.6099544	-1223.340863
5c	1.4298452	-1520.770355	-1529.180361
6c	1.7119154	-1824.93138	-1835.025859
2d	0.5039498	-456.7999742	-459.3243247
3d	0.6162941	-685.2994157	-689.0909035
4d	0.7792332	-913.7623926	-918.8190098
5d	0.9607187	-1142.212207	-1148.532485
6d	1.1510374	-1370.655701	-1378.238987
2e	0.8534442	-759.7069947	-763.9063888
3e	1.1399762	-1139.658275	-1145.962665
4e	1.4776238	-1519.573402	-1527.980972
5e	1.8343023	-1899.47505	-1909.9843
6e	2.1995462	-2279.369982	-2291.980358